Performance Study of MIL-53 (Fe) and Its Doped Variants as Potential Photocatalysts

Kamini Ishwarlal Chaudhari

Department of Chemical Engineering
National Institute of Technology, Rourkela.

Performance Study of MIL-53 (Fe) and Its Doped Variants as Potential Photocatalysts

Thesis submitted in partial fulfillment of

the award of the degree of

Master of Technology

In

Chemical Engineering

By

Kamini Ishwarlal Chaudhari

(Roll Number: 214CH1096)

based on research carried out under the

supervision of

Dr. Pradip Chowdhury

May 2016

Department of Chemical Engineering

National Institute of Technology, Rourkela.

Department of Chemical Engineering
National Institute of Technology, Rourkela

May 25, 2016

Certificate of Examination

Roll Number: *214CH1096*

Name: *Kamini Ishwarlal Chaudhari*

Title of Dissertation : *Performance Study of MIL-53 (Fe) and Its Doped Variants as Potential Photocatalysts*

We the below signed, after checking the dissertation mentioned above and the official record book of the student, hereby state our approval of the dissertation submitted in partial fulfillment of the requirements of the degree of *Master of Technology* in *Chemical Engineering* at *National Institute of Technology, Rourkela*. We are satisfied with the volume, correctness, quality, and originality of the work.

Dr. P. Chowdhury

Supervisor

Dr. P. Rath

Head of the Department

External Examiner

Department of Chemical Engineering
National Institute of Technology, Rourkela

Dr. Pradip Chowdhury
Professor

May 25, 2016

Supervisor's Certificate

This is to certify that the work presented in the dissertation entitled *Performance Study of MIL-53 (Fe) and Its Doped Variants as Potential Photocatalysts* submitted by *Kamini Ishwarlal Chaudhari*, Roll Number 214CH1096, is a record of original research carried out by him under our supervision and guidance in partial fulfillment of the requirements of the degree of *Master of Technology* in *Chemical Engineering*. Neither this dissertation nor any part of it has been submitted earlier for any diploma or degree to any university or institute in India or abroad.

Dr. Pradip Chowdhury
Assistant Professor

Dedication

To

My Loving Parents

Chandrakala Chaudhari

Ishwarlal Chaudhari

&

Special one: *Pari*

Declaration of Originality

I, *Kamini Ishwarlal Chaudhari*, Roll Number *214CH1096* hereby declare that this dissertation which is entitled as *Performance Study of MIL-53 (Fe) and Its Doped Variants as Potential Photocatalysts* presents my original work carried out as a M Tech student of NIT Rourkela and, to the best of my knowledge, contains no material previously published or written by another person, nor any material presented by me for the award of any degree or diploma of NIT Rourkela or any other institution. Any contribution made to this research by others, with whom I have worked at NIT Rourkela or elsewhere, is explicitly acknowledged in the dissertation. Works of other authors cited in this dissertation have been duly acknowledged under the sections Reference.

I am fully aware that in case of any non-compliance detected in future, the Senate of NIT Rourkela may withdraw the degree awarded to me on the basis of the present dissertation.

May 25, 2016

Kamini Ishwarlal Chaudhari
NIT, Rourkela

Contents

List of Figure

List of Tables

Nomenclature

BG	-	Brilliant Green
DMF	-	Dimethyl Formamide
DSC	-	Differential Scanning Calorimetry
FT-IR	-	Fourier Transform InfraRed spectroscopy
H_2BDC	-	Benzene dicarboxylic acid
HOMO	-	highest occupied molecular orbitals
HPMVL	-	High Pressure Mercury Vapor Lamp
LUMO	-	lowest occupied molecular orbitals
MIL	-	Matérial Institut Lavoisier
MOF	-	Metal Organic Framework
PXRD	-	Powder X-Ray Diffraction
SBU	-	Secondary Building Units
SEM	-	Scanning Electron Microscope
TGA	-	Thermogravimetric Analysis

Acknowledgment

It is customary to express our gratitude to many individuals in acknowledgement of this dissertation in most formal fashion; however, given the exceptional personalities I had come across past years and intimate relationship I enjoyed, I would like to express my sincere gratitude to all those wonderful people straight from my heart, unedited.

Dr. Pradip Chowdhury is great mentor and gifted teacher as always inspired me and cheered me up at the time of frustration with his own life experiences. The unconditional trust he had on me was the greatest of all, for I had complete freedom of expression and thought for research as well as non-research aspects. I will be indebted to him forever for all the support and care, for helping me realize my dreams.

I am very fortunate and grateful to have senior cum friend Mr. Prince George for his unconditional assistance, encouragement and discussions that made way to generate new exceptional ideas for work. I hope at least now he will get “the peace of mind”. Also I thank all my lab mates Nikhil Dhabarde, Prashant Niture and Vikas Kumar for all their support.

I am thankful to Dr. P. Rath, HOD, and all faculties of chemical engineering department for support and facilities, made available. I would like to thank National Institute of technology for giving the opportunity for research.

Last but not the least, to my lovable parents, I. C. Chaudhari and C. I. Chaudhari and adorable siblings, for incredible love and support and for the believing me unconditionally in what I do, 1600 kilometers away from institute during my course.

25th May, 2016 **Kamini Chaudhari**

Rourkela

Abstract

This work includes synthesis of MIL-53 (Fe) metal organic framework and its doped derivatives (Li, Na, K) using microwave technique. Various characterization techniques like SEM, PXRD, TGA, FT-IR and UV-Vis reflectance detailed the physical, thermal and electronic properties of the synthesized materials. MIL-53 (Fe) was found to be stable up to 330°C and fairly stable in aqueous environment where pH was ranging from 2-11. MIL-53 (Fe) along with its cation doped variants were found to be photocatalytically active and the activity decreased in the following order: MIL-53 (Fe) > MIL-53 (Fe) Li > MIL-53 (Fe) K > MIL-53 (Fe) Na; both in presence as well as in absence of an electron acceptor (H_2O_2). MIL-53 (Fe) showed degradation efficiency of approximate 86% and in presence of H_2O_2 as an enhancer it was increased to 96%.

Keywords: MIL-53 (Fe); characterization; photodegradation; Photosensitivity; Optimization.

CHAPTER 1

INTRODUCTION

It has been a dream of scientist to build chemical structures from molecular building blocks and this idea came to fulfill after the invention of Metal Organic Frameworks. It is generally acknowledged that MOFs exhibit unique and outstanding properties, which have been discussed in various reviews. The fact has been exploited by researchers about finding of more than 2000 MOF structures. Metal Organic Frameworks (MOFs) are highly crystalline hybrid compounds built up of the inorganic metal ions or clusters (i.e. secondary building unit, SBU,) say d-transition element like Ti, Cr, Fe, Mn, Co, Ni, Cu etc. and organic linkers like BDC, BTC, DABDC, NDC etc., connected by coordination bonds of moderate strength. MOFs are having the special properties of large surface area and pore volume. MOFs coordination polymers have received great attention due to their many potential applications ranging from catalysis, gas absorption, optics, energy storage, molecular recognition, drug delivery and so on [1]. The interest in the area of photocatalysis is due to their fascinating structures and many possible metal ligand co-ordinations, as well as the aforementioned properties, including band gap are tunable by differing the building blocks and reaction conditions. My work is based on application of synthesized MOFs (MIL-53(Fe) and its doped variant) in enormous area of photocatalysis by degrading an organic dye *viz.* Brilliant Green (BG).

Naturally, the photo excitation of electrons resulting conversion of solar energy into chemical energy has been materialized by green plants and the process is well known as photosynthesis. Many solids that yield enhanced number of electron-hole pairs at their surface when illuminated by radiation in the visible or ultraviolet regions of the spectrum are known to exhibit the phenomenon of photocatalysis. The entire structural geometry of MOFs is composed of ligands-SBU interfaces where SBUs are the ionic or oxide centers. Hence the electronic properties of MOFs can be influenced by the interfacial energy level realignments at these interfaces. This feature makes it possible to chemically tuning the bulk electronic

properties of the MOF by exchanging SBUs and linkers, facilitating the way for exploring the MOFs as a new group of semiconducting materials. Theoretical calculation have shown that the band gaps of MOFs are difference between the LUMOs (lowest occupied molecular orbitals) and HOMOs (highest occupied molecular orbitals) of the organic linkers. The band gap energy can be controlled between 1.0 to 5.5 eV via ligand functionalization [2]. It is also known fact that it is possible to tune the band gaps of MOF based semiconductor materials by altering the dimensions of the metal cluster SBUs.

The use of solar energy for removal of organic pollutants from various industrial and domestic sources is a known concept and photocatalysis is one of the mechanisms towards achieving that. The first artificial photocatalyst *viz.* TiO_2 was successfully used in pollutant degradation and eventually many metal sulfides and oxides including CdS, ZnS, ZnO, have been identified as active photocatalysts for photo degradation of pollutants in aqueous and gas phase [3, 4]. As many of these photocatalyst are nonporous in nature resulting less surface area, the solar energy conversion efficiency of those photocatalysts are low, their practical application remains largely limited hence the MOFs have the large scope in photocatalysis.

Many strategies have been adopted to improve the photocatalytic activity and photo corrosion resistance of semiconductors; e.g. tailoring the particle morphology and surface reaction sites, band-structure modification using impurity doping and loading of a noble metal cocatalyst, controlling the charge transfer dynamics using composite semiconductors [5]. A special method to introduce dopants to the semiconductor lattice to form an efficient composite semiconductor is widely used to tune the band gap of semiconductor.

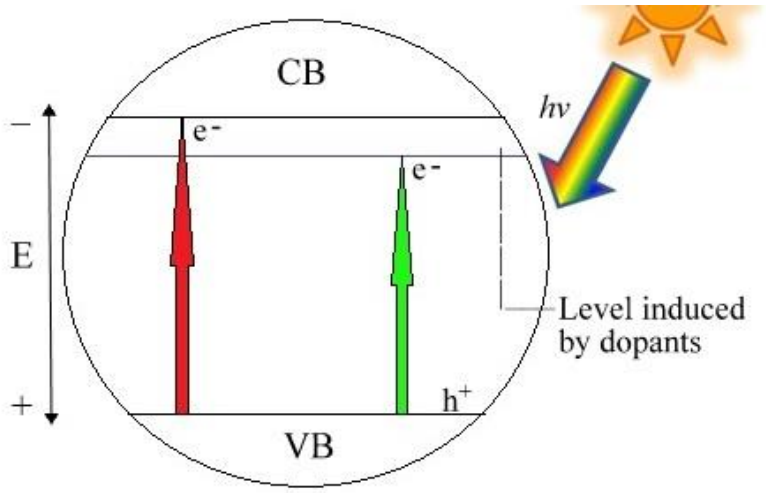

Figure 1.1: Schematic of cation doping to a semiconductor.

Cation doping is able to influence the behavior of a photocatalyst in such a way that it becomes active under visible light. It does this lowering the conduction band of the semiconductor. Cation can serve as recombination centers since they so readily accept electrons. To overcome this problem, the doping of anions has been investigated. Anion doping increases the valance band of the semiconductor.

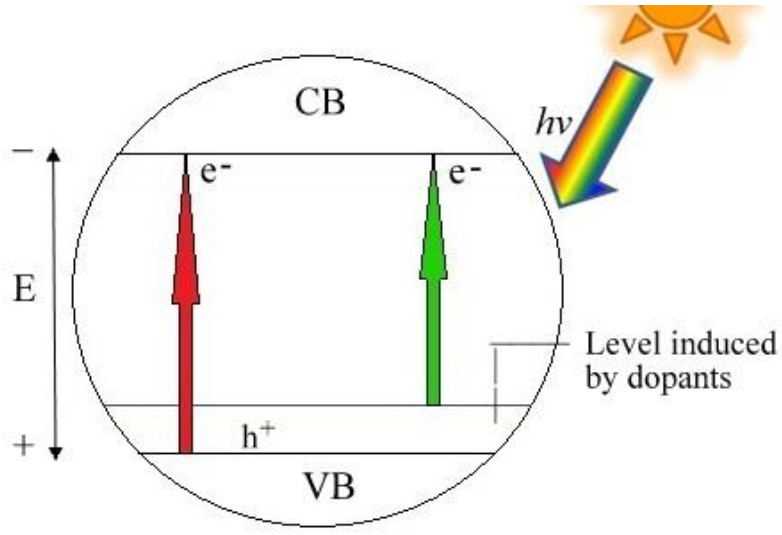

Figure 1.2: Schematic of anion doping to a semiconductor.

A dye is a colored substance which has an affinity to the substratum to which it is being applied. Some dyes used in industries are toxic, carcinogenic, or may cause higher risk of tumors if come in contact with human body. MOFs may have a wide application in

degradation or decolorization of dyes. The part that is the cause for color into a dye molecule is known as a chromophore. The chromophore is an aromatic structure containing benzene, naphthalene, or anthracene. Groups from a donor chromophore color are represented by the following radicals: azo (- N = N -), carbon (= C = C =), carbonyl (= C = O), carbon-nitrogen (> C = NH - CH = N -), nitric (- NO2 or = NO - OH), nitro (- NO or N - OH), and sulfide (> C = S, carbon-sulfur). Various dyes from different groups were selected for degradation over MIL 53 (Fe) photocatalyst.

BG dye is odorless yellow-green to green powder used for biological staining, veterinary medicine, and an additive in poultry feed. It is also extensively used in textile and paper printing industries. Various methods have been used to build up effective methodologies for removal the said dye. BG is a cationic dye which is characterized in triarylmethane dyes. It is highly toxic induces vomiting when swallowed and release harmful gases if tried to degrade by heating. However, no single technique is being suitable yet for treatment of this stubborn dye.

Optimization has been done by implementing the TAGUCHI optimization model to the experimental data. Taguchi method is a statistical technique which allows one to improve the consistency of production of a particular product. Taguchi designs recognize that all factors that are cause of variability cannot be controlled and these factors are called noise factors. These designs try to identify the controllable factors that minimize the effect of noise factors. During experimentation control factors are manipulated to evaluate variability that occurs and optical control factor settings that minimizes the process variability are determined. The process designed with this goal will produce more consistent output and performance regardless of the environment in which it is used. Now a days this statistical technique is used in many areas like engineering, biotechnology, marketing and advertising and so on.

Research objectives

a) Synthesis and characterization of MIL-53 (Fe) and its doped variants
b) Studying aqueous phase stability of synthesized MOFs
c) Photo degradation of Brilliant Green dye using synthesized catalysts
d) Optimization of the photodegradation process

Thesis summery

The complete thesis has been organized in 5 chapters. **Chapter 1** (Introduction) defines the basic chemistry of metal organic framework and explains about application of MOF in photo catalysis. It also highlights the research objectives. **Chapter 2** (Literature review) gives the detailed review about MOFs synthesis and their application in various fields. **Chapter 3** (Materials and methods) consist systematic explanation of material synthesis and their characterization. In this section detail protocol followed for photocatalytic applications and optimization is documented. **Chapter 4** (Results and analysis) gives reasoning on all experimental results with perticular references, systematically. **Chapter 5** (Conclusion and Future scope) concludes the research findings and highlights the extension of this present research work.

CHAPTER 2

LITERATURE REVIEW

In literatures current study deals with not only synthesis but also structure of 3 novel coordination polymers that has been taking out by employing hydrothermal methods, by Partha Mahata et al in 2006. The samples have been analyzed using a multiplicity of techniques for instance powder XRD, FT-IR, UV-vis, photoluminescence, magnetic, and photocatalytic studies. All the compounds emerge to be active for the photocatalytic decay of ordinary organic dyes used in textile industries, with activities better than Degussa P-25 TiO_2 catalysts. Author helped to propose a probable mechanism, through an activated complex involving M^{+2}. This study undoubtedly expose that it is advantageous to examine metal carboxylate for photocatalytic activity [7].

Researchers Francesc X. Llabres i Xamena et al discussed about MOFs application as Quantum Dot Semiconductors in 2007. Right through this contribution, they have represented preface, up till now very hopeful, result that display the potentialities of metal-organic hybrid solids as optoelectronic materials i.e. an area that has not been reflected on so far. These comprise photocatalysis with reverse shape-selectivity, photovoltaic solar cells, and electroluminescence devices. The outcomes illustrated here for these applications are still far from the performance of state of the art mechanisms planed with predictable materials.

On the other hand, it is understandable that substantial quantities of work have been carried out advancing and optimizing the efficiency of standard semiconductors for their application in photovoltaic cells, photocatalysis, and electroluminescence. On the contrary to this, the results presented by this research pass on to a novel material that has not even been used in these areas. But known the adaptability of metal organic hybrid materials, much improvement can also be achieved for those materials, as summarized within the text. Also, it can be anticipated that metal-organic hybrid materials are certainly not restricted to the above-stated applications and that new properties based on the quantum dot-organic photo sensitizer combination can be predicted for this expanding class of hybrid materials [8].

Present research David Farrusseng et al deals with Opportunities of MOFs as a catalyst. Author basically sited his concentration on their assets and restriction in light of present confronts in catalysis as well as green chemistry. Catalytic functions are used to represent not only their structural but also dynamic features in conjunction with MOFs designing to fulfill the gap between zeolites and enzymes. The participation of MOFs in the area of catalysis is broadly investigated and a list of catalytic contenders is provided. The area under discussion is presented from multidisciplinary opinion enveloping solid-state chemistry, materials science, and catalysis [1].

From the study of present researches, author observed that catalytic applications by means of MOF materials generally experience lack of characterization with regard to sample homogeneity and purity. Almost only X-ray diffraction (XRD) method is used for the analysis, even though little extents of unstructured metal oxide phases or other crystalline phases present can be liable for the catalytic activities observed.

Research study of B. Ohtani gives us brief idea about Photocatalysis. He distinguished properties related to photocatalysis as well as photo-electro-chemical reactions in alphabetical approach such as Activity, Band structure and Crystallinity to X-ray photoelectron spectroscopy, Yield and Z-scheme photocatalysis with clarification of what what we do not know in a scientific sense.

Study also helps in one more important point which is to be familiar with the distinction between either “necessary” conditions or “sufficient” conditions. As is frequently the case, an experimental outcome seems to be evidence of a certain assumption, when the result is just the same as that expected. However, outcomes are always needed conditions and illustrate prospect of the assumption. This is not only important in photocatalysis but scientific studies also require such reflections [4].

Chi-Kai Lin et al study deals with the special property of the MOFs i.e. tunability of band gap. In review, researcher made obvious that the band gap tunability of MOFs can be accomplished via two different policies that are varying the cluster size of metal ligands and shifting the conjugation of the organic linker. Author is also continuing his work i.e. either on further increase of the size of SBUs or the π conjugation of the organic ligands can further narrow MOFs’ band gap. In point of view, it is identified that many aspects can also

contribute to the band-gap shift in the semiconducting nano-clusters counting cluster size, electronic effects such as electron-phonon coupling, vacancies, shape effect (principally at small sizes), and other surface defects and so on [8].

From authors' point of view, the impact on MOF's band gap by SBU is going to be more difficult than what they have conferred in this research; this will help only as starting point. Such complication, on the other hand, more opportunities are also recommended to further tuning of the electronic and optical properties of MOFs via new SBU design to find useful applications in the fields of electronics and optics.

Yanghe Fu et al (2012) study represents reduction of CO_2 to $HCOO^-$ under visible light irradiation with the help of photocatalyst is for the first time comprehended over a photoactive Ti build MOF, NH_2-MIL-125 (Ti), which is manufactured by a superficial replacement of ligands in the UV-responsive MIL-125 (Ti) material. This study briefly discusses the prospective of MOFs as photocatalysts for the reduction of CO_2. Even though the activity for the reduction of CO_2 over the present NH_2-MIL-125 (Ti) catalyst is still low, considering the adaptable coordination chemistry of the metal cations, the accessibility of different organic linkers, and the opportunity to modulate the composition, structure, and properties of the MOFs, authors accept as true that high-efficient MOF-based photocatalysts for the reduction of CO_2 can be gained. A restriction in the current photocatalytic system is that TEOA has to be employed as the sacrificial electron donor, which is not commercial as well as environment friendly. This research helps to recommend a solution to this problem by recycling the sacrificial amine by coupling the photochemical reduction of CO_2 to a photochemical water splitting reaction. Even if most of the reported MOFs cannot prolong the water oxidation process, some are moderately stable in water. Consequently, the photocatalytic cycle is absolute and the MOFs-based photocatalysts to reduce CO_2 in the existence of a recyclable amine as electron donor under solar irradiation [10].

Study of P V Korake et al deals with cation doping of nano crystalline CdS for production of hydrogen from water. Study was intended at judicious enhancement in the visible light driven water splitting activity of nano crystalline CdS photocatalysts on account of their doping with a small amount of an aliovalent cation (Ag^+ or Cr^{3+}). One step hydrothermal method was used to synthesize required samples which were analyzed systematically for their morphological,

crystallographic, interfacial, and photo-physical properties. Rietveld refinement and X-ray powder diffraction data is used for quantification of the doping effect on the phase composition as well as lattice parameters.

Researcher come up with the result as, on comparison with pure CdS, the samples including ~0.2 weight % of Cr or Ag confirmed two or tenfold enhancement in the rate of H_2 evolution from water in presence of sulfide - sulfite ions as sacrificial electron donors. They also conclude that pyramidal trend, i.e. utmost activity for specific contamination content, which reduced not only on decreasing but also on increasing the amount of doping, did not suggest itself due to the presence of a secondary phase metal sulfide or a dispersed metal co-catalyst. Current study naked that instead of the widely adapted mechanism involving either inter-semiconductor or semiconductor for metal electron relocate steps, the doping helps to modify photo action of CdS which was governed by certain bulk and surface properties for instance the cation-dependent particle nucleation, dominance of hex-CdS facets, and structural defects. Furthermore, impurity-induced, sub-bandgap, charge-trapping states also contributed to the overall quantum efficiency [12].

CHAPTER 3

MATERIALS AND METHOS

3.1 Chemicals and reagents used

All chemicals were analytical grade and used without further purification. 96% Iron (III) chloride anhydrous purified (Merck), 98% Terephthalic acid pure (LOBA Chemie), 99% N, N-dimethylformamide (Emplura). Lithium Acetate (99%) (LOBAChemie), Sodium Acetate (98%) (Fisher Scientific), Potassium Chloride (99.5%) (Fisher Scientific), Iron (II) chloride anhydrous (97%) (Merck), Hydrogen Peroxide (30% w/v) (Fisher Scientific), Urea extra pure (99.9%) (SDFC ltd). De-ionized water obtained from a Millipore Milli-Q system was used to prepare aqueous solutions for synthesis and for the irradiation experiments. Dyes like Methylene Blue, Brilliant Green, Congo Red, Remazol Golden Yellow, Trypan Blue, Amido Black.

3.2 Instrumentation utilized

MOFs were synthesised using microwave reactor (Monowave 300, Anton Paar).

Characterization of the sample was performed using SEM, Powder XRD, TGA, UV Diffused reflectance and FT-IR. The morphologies of synthesized materials were observed via scanning electron microscopy (SEM, JEOL JSM-6480 LV) equipped with an energy dispersive X-ray spectrometer (EDS). Prior to imaging, each sample was Au/Ag coated for better imaging. The synthesized samples were subjected to X-ray diffraction by a diffractometer (XRD, Philips Analytical, PW-3040) equipped with the graphite monochromatized Cu Kα radiation (λ=1.5406Å) in 2θ angles ranging from 5^{o} to 50^{o} with a step size of 2 degrees and scanning rate 1^{o} per minute. Thermal stability of samples was carried out in detail in a TGA apparatus, Shimadzu (DTG 60 H). UV Diffused reflectance was carried out using UV-Vis spectrophotometer with integrated sphere (JASCO-750). And FTIR was performed in ThermoFicher Nicolate IS-10, from 500cm^{-1} to 4000 cm^{-1}with bandwidth of 0.5 nm.

For analyzing dye concentrations for photocatalytic experiments UV-Vis spectrophotometer (JASCO -750) was employed.

3.3 Optimization for Synthesis

3.3.1 MIL-53 (Fe)

In a typical preparation, a solution of $FeCl_3$ (2.433 g; 15 mmol) and 1, 4-H_2BDC (2.492 g; 15 mmol) in N, N-dimethylformamide (150 mL) was poured into a vessel. This vessel was placed on magnetic stirrer and stirred for approximately 2 hr. The resulting mixture solution was then transferred into a microwave reactor and heated to various temperature and holding time for optimization as given in the table.

Table 3.1: Optimization parameters for synthesis of MIL-53 (Fe)

Temperature (ºC)	Holding Time (min)
70	120
100	14
120	15
150	10

The obtained product was re-suspended in DMF and stirred for 12 hours for purification. After centrifuging again, at 6000 rpm for 15 minutes, it was kept for drying in a hot air oven at 150 ºC for overnight and allowed it to cool at room temperature. The solid was then stirred in deionized water (3 g of MIL-53 (Fe) in 1000 ml of water) twice to remove traces of ultrafine particles and DMF.

3.3.2 Doped variants of MIL-53 (Fe)

Same procedure has been followed for synthesis of Na doped MIL-53 (Fe) (by adding Sodium Acetate instead of Lithium acetate), and K doped MIL-53 (Fe) (by adding Potassium Chloride instead of Lithium acetate) for stirring time 30 min, 4 hours, 8 hours. All samples are stored safely for characterization.

Table 3.2: Optimization parameters for synthesis of MIL-53 (Fe) derivatives

Material Synthesized	Stirring Time		
	Min	Hrs	Hrs
Li doped MIL-53 (Fe)	30	4	8
Na dope MIL-53 (Fe)	30	4	8
K doped MIL-53 (Fe)	30	4	8

3.3.3 α-Fe_2O_3

The solution of $FeCl_3$ (1 M) and urea (1 M) are mixed and heated at 90 ºC for 2 hours. The resulting product contains hydroxyl iron oxide and Ammonium chloride. This product is centrifuged and dried in hot air oven. Ammonium chloride is a sublimate hence it will get evaporate during dying leaving behind hydroxyl iron oxide which is sintered at 240 ºC for 2.5 hrs to obtain α-Fe_2O_3. This red brown powder of α-Fe_2O_3 is store safely in vacuum desiccator.

3.3 Aqueous interaction of MIL-53 (Fe)

Synthesized MOF (MIL-53 (Fe)) was weighed and added to the equal quantity of deionized water (30 ml) with variable pH conditions (i.e. 2, 4, 7, 9 and 11) in separate 30 ml tubes. The pH of aqueous mediums was maintained using standard buffer solutions. The accurate pH values were measured using glass electrode pH meter. Samples are stirred using magnetic stirrer for about 4 hours at room temperature. Then the suspension is centrifuged at 6000 rpm, 15 minutes and dried in hot air oven at 150 ºC separately and stored for further characterization.

3.4 Photo catalytic activity of material

The aqueous solution of Methylene Blue of 7.5 ppm was prepared and was standardized at various concentrations of MB and de-ionized water. The standardization results are reported in Appendix I. Photocatalytic activity of α-Fe_2O_3, MIL 53 (Fe), Li doped MIL-53 (Fe), Na doped MIL-53 (Fe), and K doped MIL-53 (Fe) photocatalyst was estimated by photodegradation of Methylene Blue (MB) dye under High Pressure Mercury Vapor Lamp i.e. HPMV Lamp (125W). The schematic diagram of experimental set up for measurement of photoactivity and photodegradation is given in figure below.

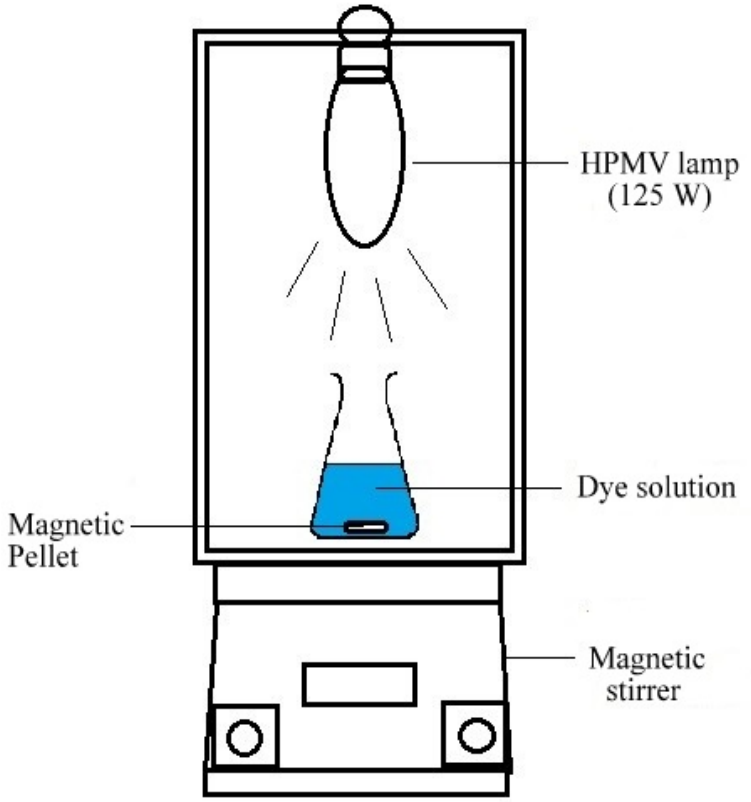

Figure 3.1: Schematic diagram of experimental set up

The distance between the light source and the beaker containing reaction mixture was fixed at 20 cm. A known quantity of MOF sample was measured in scintillation flask of 30ml and known quantity of dye aqueous solution was added to the flask. The pH of the suspension was adjusted to be neutral (pH 7.0). Prior to irradiation, the suspension was magnetically stirred in dark for 30 minutes to ensure the establishment of adsorption equilibrium. Stirring was maintained to keep. the mixture in suspension during the entire duration of photo degradation experiment. Solution was irradiated after 30 minutes of adsorption and samples were withdrawn at regular intervals. The samples were immediately centrifuged to separate photocatalyst and the supernatant was analyzed using UV visible spectrophotometer. The experiment was carried out for a duration of 2 hours. The absorbance at maximum wavelength (λ_{max}) was measured to monitor the dye concentrations using a UV-visible spectrophotometer in a 1 cm path length spectrometric quartz cell.

3.5 Test for Photosensitivity of dyes

Photosensitivity was studied by irradiating various dyes under HPMV Lamp (125W) without addition of catalyst. Two reaction mixture were prepared and irradiated. One, control i.e. dye solution alone. Second being dye solution plus an oxidant (i.e H_2O_2). The samples were immediately analyzed using UV visible spectrophotometer. The experiment was carried out for a duration of 2 hours. The absorbance at maximum wavelength (λ_{max}) was measured to monitor the dye concentrations using a UV-visible spectrophotometer in a 1 cm path length spectrometric quartz cell. Substrates studied for photosensitivity were Brilliant Green, Congo Red, Remazol Golden Yellow, Trypan Blue and Amido Black.

3.6 Photodegradation of BG dye using photocatalyst

BG dye was degraded over synthesized materials *viz.* MIL 53(Fe), Li doped MIL-53 (Fe), Na doped MIL-53 (Fe), K doped MIL-53 (Fe) and α-Fe_2O_3. A known quantity of MOF sample was measured in scintillation flask of 30ml and known quantity of dye aqueous solution was added to the flask. The pH of the suspension was adjusted to be neutral (pH 7.0). Prior to irradiation, the suspension was magnetically stirred in dark for 30 minutes to ensure the establishment of adsorption equilibrium. Stirring was maintained to keep the mixture in suspension during the entire duration of photo degradation experiment. Solution was irradiated after 30 minutes of adsorption and samples were withdrawn at regular intervals. The samples were immediately centrifuged to separate photocatalyst and the supernatant was analyzed using UV visible spectrophotometer. The experiment was carried out for a duration of 2 hours. The absorbance at maximum wavelength (λ_{max}) was measured to monitor the dye concentrations using a UV-visible spectrophotometer in a 1 cm path length spectrometric quartz cell.

The effect of enhancer on photodegradation was studied by following the above mentioned protocol.

3.7 Optimization of photodegradation

After analyzing the results of photodegradation of BG dye by synthesized photocatalysts, it was decided to optimize the degradation by varying 3 parameters i.e. dye concentration (3

ppm, 6 ppm, 10 ppm, 15 ppm, 20 ppm), enhancer concentration (0 mM, 0.1 mM, 1 mM, 10 mM, 50 mM) and catalyst weight (0 mg, 5 mg, 10 mg, 20 mg, 25 mg) and variables, shown in brackets, to obtain the best combination for photodegradation of BG dye solution. DOE on level III were carried out via TAGUCHI optimization model best one chosen on the response of photodegradation.

CHAPTER 4

RESULTS AND DISCUSSION

4.1 Bulk synthesis of MIL-53 (Fe) and its doped variants

Table 4.1: Results of optimization of Temperature and holding time for MIL-53 (Fe) synthesis

Temperature (ºC)	Time (min)	Results (Observation)
70	120	Clear, no suspension
100	14	Slightly turbid, No ppt
120	15	Orangish yellow ppt
150	10	Dark Red Orange ppt

From above observations in table 4.1, synthesis of MIL-53 (Fe) is carried out at temperature 120 ºC and holding time 15 minutes. After the reaction, the resulting Orangish yellow suspension was centrifuged and purified. The obtained product was orange crystal powder. Synthesis of Li doped MIL-53 (Fe), Na doped MIL-53 (Fe), K doped MIL-53 (Fe) at stirring time 8 hours gave good quality of crystal and better quantity compared to 30 min and 4 hour stirring time. Hence all 3 MOFs are synthesized in bulk after 8 hours of stirring time.

4.2 Characterization

Prepared MIL-53 (Fe) and MIL-53 (Fe) doped with Li, Na, and K were analyzed by SEM, PXRD, TG Analysis, UV Reflectance Analysis and FTIR. The proper explanation of morphology and structure of synthesized material are detailed below.

4.2.1 SEM analysis

Surface morphology studies are considered to be the primary evidence for formation of any required sample before any chemical or physical analysis. Hence the surface morphology was studied under Scanning Electron Microscope (SEM) for synthesized materials and are shown

in figure 4.1. The SEM image shown in Figure 4.1 (A) depicts synthesized MIL-53(Fe) with octahedral morphology as found in literature [7][14].

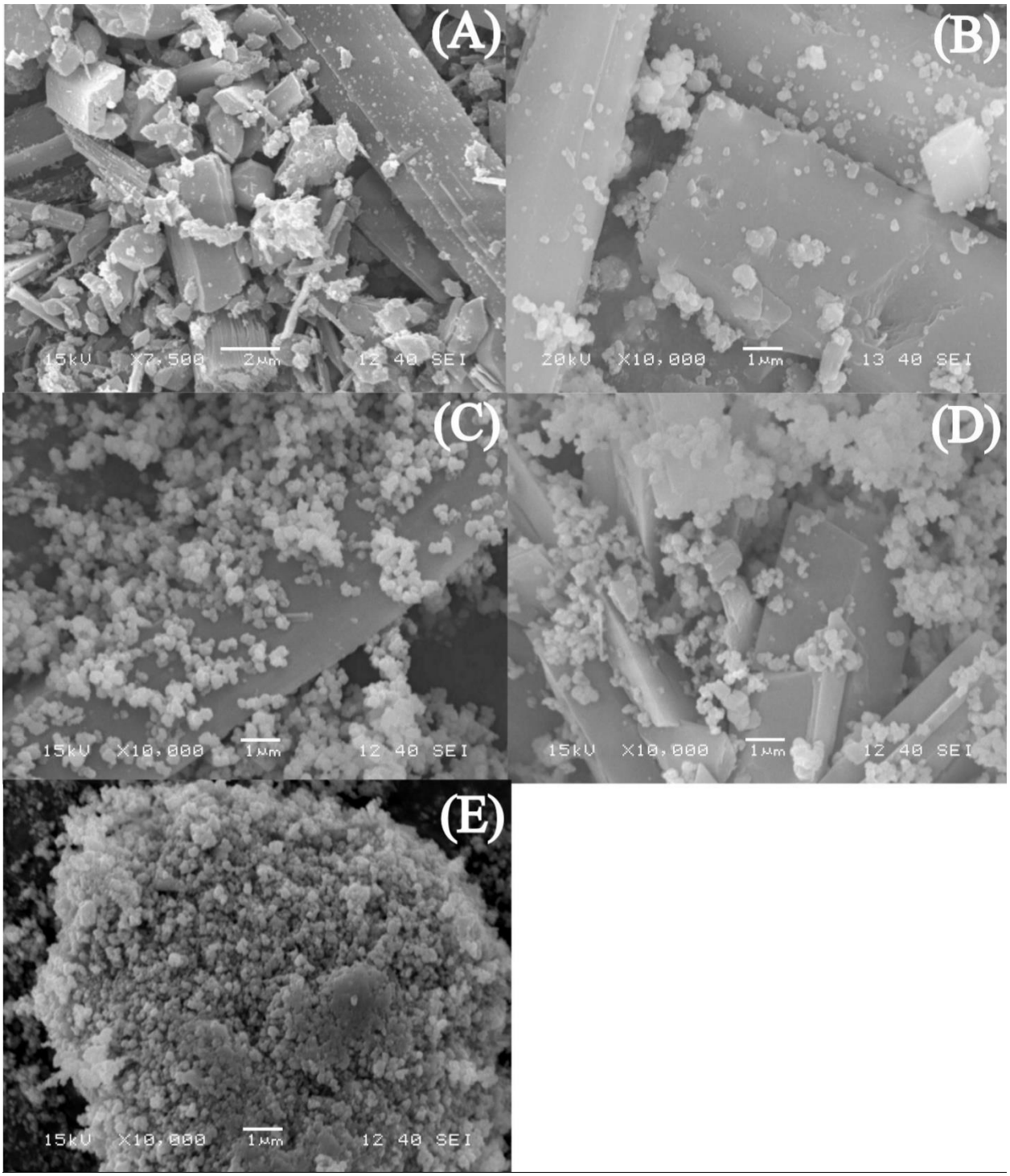

Figure 4.1: SEM images of (A) MIL-53 (Fe), (B) MIL-53 (Fe) Li doped, (C) MIL-53 (Fe) Na doped, (D) MIL-53 (Fe) K doped (E) α-Fe_2O_3

From the Figure 4.1 (B) (C) (D), similar crystal morphologies for the MIL-53 (Fe) doped variants was clearly observed. With increase in initial reaction time fine MOF crystal formation can be explained due to the formation of proto MOFs in the initial stages of nucleation and crystal growth. The synthesized α-Fe_2O_3 shows crystalline morphology as found in literature with particle size ranging from 0.7-1.0 µm.

4.2.2 PXRD Spectra of MIL 53 (Fe) and its doped variants (Li,Na,K)

The Powder X-Ray Diffraction patterns depicts that the synthesized MOF (MIL 53 (Fe)) and its dopants such as Li, Na, K were in crystalline form. From PXRD spectra shown in Figure 4.2 it was found that the 2θ positions for synthesized material are matching with the appropriate 2θ positions for MIL 53 (Fe) from the literature data confirming that the synthesized material is MIL 53 (Fe) [7] [14].

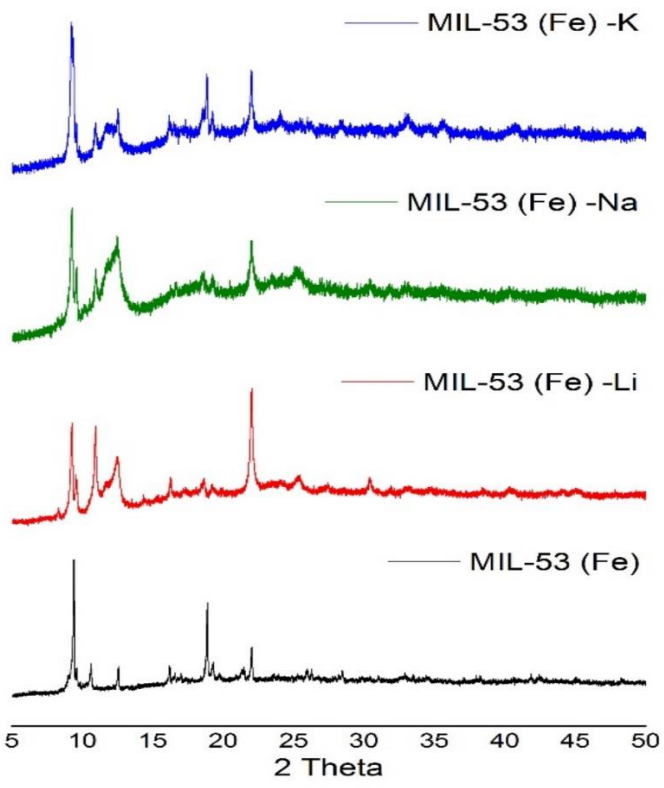

Figure 4.2: PXRD of MIL-53 (Fe), MIL-53 (Fe) Li doped, MIL-53 (Fe) Na doped, MIL-53 (Fe) K doped.

From Figure 4.2, for MIL-53 (Fe) doped variants showed metal cation incorporation in the MOF crystal lattice. The Incorporation of cations remain consistent 2 theta positions of 10° - 15° for all the doping carried out. Showing that the cation insertion occurred in the similar lattice positions.

4.2.3 TG Analysis of MIL 53 (Fe)

Thermo Gravimetric Analysis (TGA) provides the information about thermal stability of the specific sample. Figures 4.3 and 4.4 show the TGA profile and DCS profile of MIL 53 (Fe) and its doped variants. These profiles clearly depict that MIL 53 (Fe) is thermally stable up to about 400 ºC and starts degrading after 400 ºC because of BDC oxidation process. The positive picks in DSC profile shows that the degradation of synthesized MIL-53 (Fe) is an exothermic reaction which occurs in between 400 to 425 ºC. MIL 53 (Fe) Li doped, MIL 53 (Fe) Na doped, MIL 53 (Fe) K doped are stable up to 330 ºC. Fractional weight loss between room temperature to 120 ºC is due to water removal in the material. Fractional weight loss between 120 ºC to 155 ºC is due to DMF removal as its boiling point is 150 ºC. After 330 ºC BDC is oxidized hence degradation of MOF occurs.

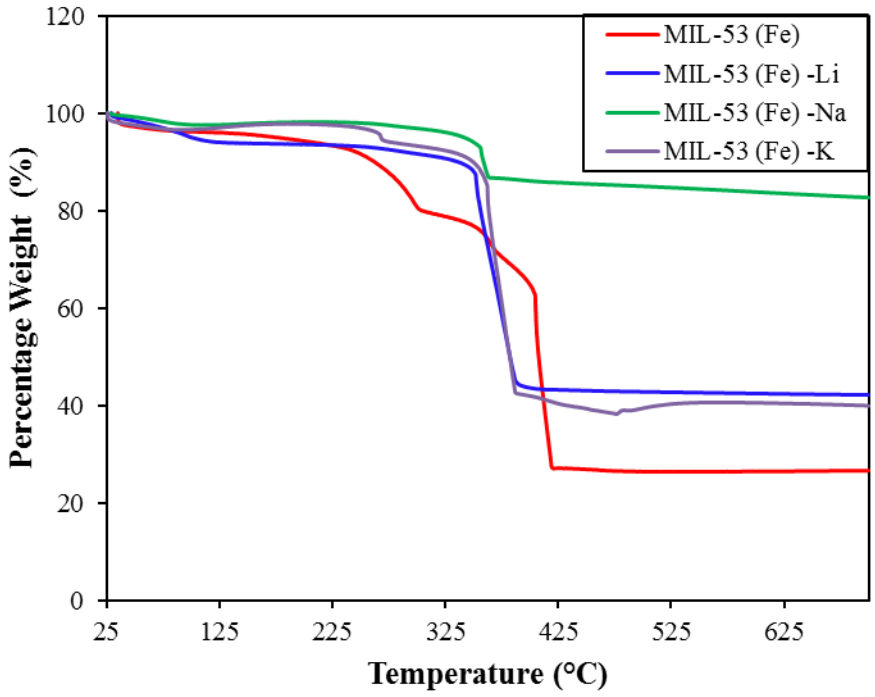

Figure 4.3: TGA profile for synthesized MOFs

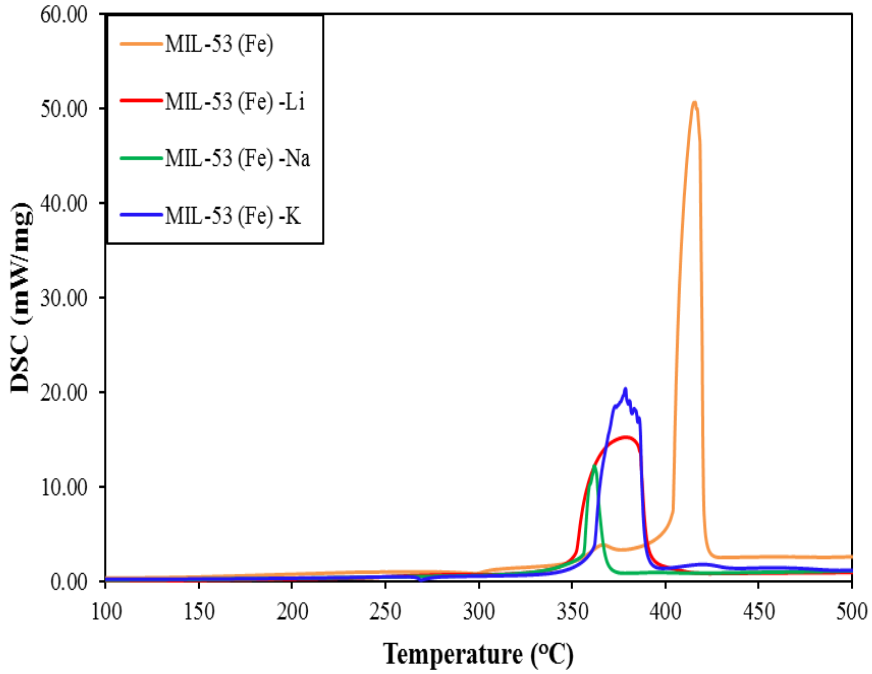

Figure 4.4: DSC profile for synthesized MOFs

4.2.4 UV Reflectance Analysis

The wavelength range under study was the UV-visible region of electromagnetic spectrum. The calculation details for band gap measurement was on the basis of K-M model. Followed by the application of Kubelka –Munk transformation of reflectance.

$$K = \frac{(1 - R)^n}{2R} \quad \text{..... (4.1)}$$

Where, K is the reflectance transformed according to Kubelka –Munk, R is the reflectance and n = 2, for direct electronic transition.

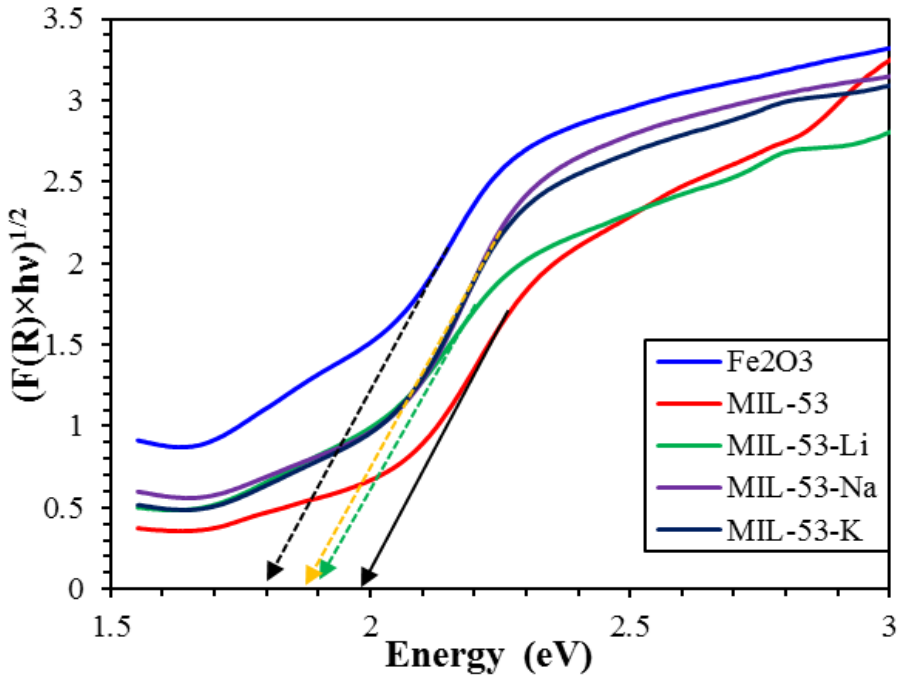

Figure 4.5: Tauc plot of synthesized MOFs and α-Fe_2O_3.

Table 4.2: Band gap energy and Threshold wavelength of different synthesized MOFs

Sr. No.	Synthesized Material MOFs	Band gap energy (eV)	Threeshold wavelength (nm)
1	MIL-53 (Fe)	2	620
2	Li doped MIL-53 (Fe)	1.9	652.6
3	Na doped MIL-53 (Fe)	1.85	670.3
4	K doped MIL-53 (Fe)	1.85	670.3
5	α-Fe_2O_3	1.8	688.9

Table 4.2 in combination with figure 4.5 showing band gap energy and threshold wavelength of the synthesized MOFs. It can be observed, band gap energy is decreases with doping. It can be understood from the figure that the increase in cation size decreases the band gap energy up to an extent. Hence the change in band gap energy can be represented in the form of Li > Na = K.

$$E_g = \frac{hc}{\lambda_{Thd}} = \frac{1240}{\lambda_{Thd}} \quad \text{..... (4.2)}$$

Where, E_g is the band gap energy, h is the Planck's constant, c is the speed of light and λ_{Thd} is the threshold wavelength.

4.2.5 FT-IR Analysis

Figure 4.6 shows FT-IR spectrum of MIL-53 (Fe), MIL-53 (Fe) Li, MIL-53 (Fe) Na, MIL-53 (Fe) K. FT-IR spectrum for MIL-53 (Fe) exhibited in the presence of strong peak 1415 cm^{-1} which is lower than the value for the C=O stretching vibration observed in free carboxylic acids. This strong peak was due to stretching vibration of carboxylate anions present in the material. The presence of strong absorption band at 931 cm^{-1} shows free hydroxyl interaction in structure. This could be due to the presence of hydrogen bonds between water molecules. The presence of Fe-O bonds and M-O (M refered to Metal cations like Li, Na, K) bonds were observed in the range above 780 cm^{-1}.

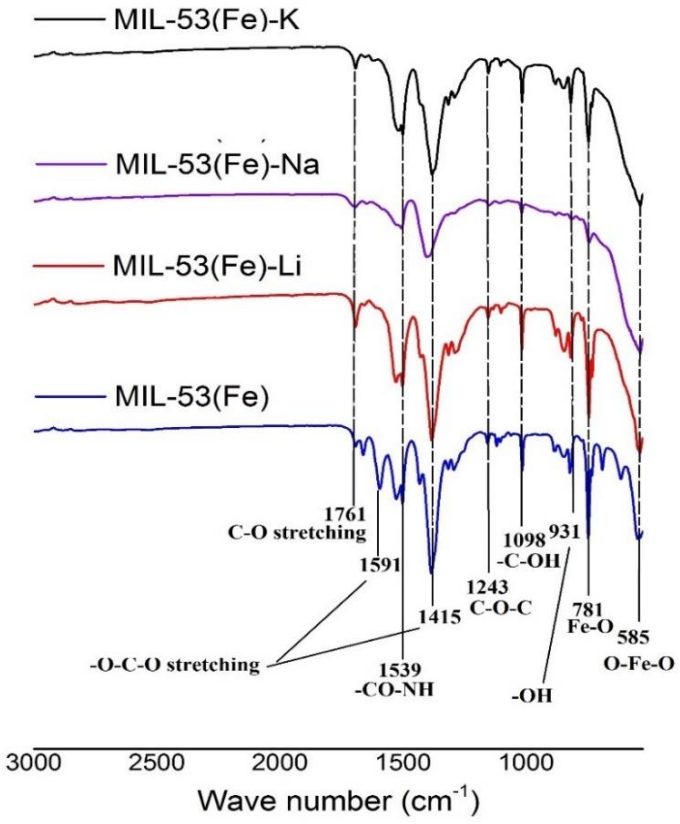

Figure 4.6: FT-IR spectrum of synthesized MOFs

4.3 Aqueous interaction results

Experimental study of aqueous stability of MIL-53 (Fe) at various pH environment results that MIL-53 (Fe) is stable in all pH ranges. Figure 4.7 and 4.8 gives the physical appearance of MIL-53 (Fe) after pH interaction and the inference obtained from the PXRD pattern. The studies showed that the MIL-53 is one of the robust material that can be employed for wide range of applications ranging from the field of heterogeneous catalysis to drug delivery.

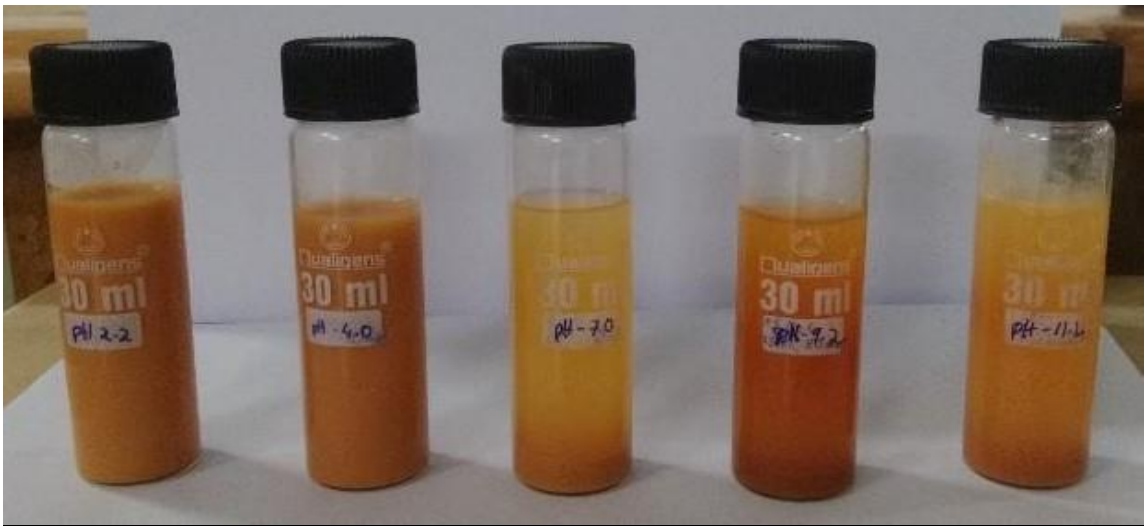

Figure 4.7: photographic view as a result of aqueous interaction of MIL-53 (Fe) at different pH environments after experiment.

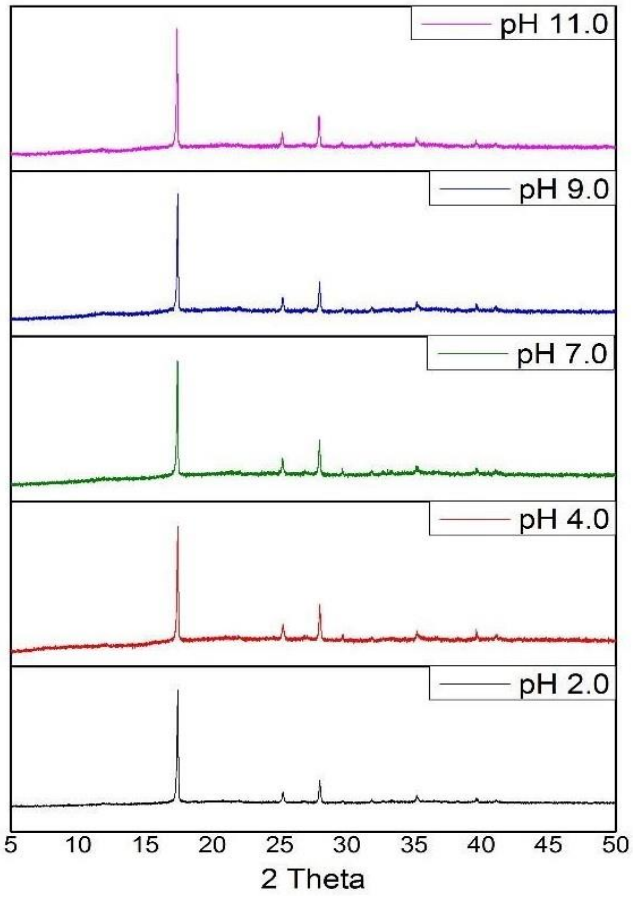

Figure 4.8: PXRD spectra of MIL-53 (Fe) after aqueous interaction.

4.4 Photo catalytic activity of synthesized material

The photocatalytic activities of four materials that are MIL-53 (Fe) and its three cation doped variants were monitored from the variation of the color in the reaction system by measuring the maximum absorbance intensity of MB chromophore group at λ_{max} 664 nm. Figure 4.9 illustrates the photo degradation profile of MB over MIL-53 (Fe) photo catalyst under the UV–vis and visible light irradiation. Notably, MIL-53(Fe) shows a comparable activity to its doped variants under UV–vis light and visible light irradiation. No MB degradation was observed over MIL-53 (Fe) photo catalyst without the light irradiation but active adsorption of MB occurs about 28%.

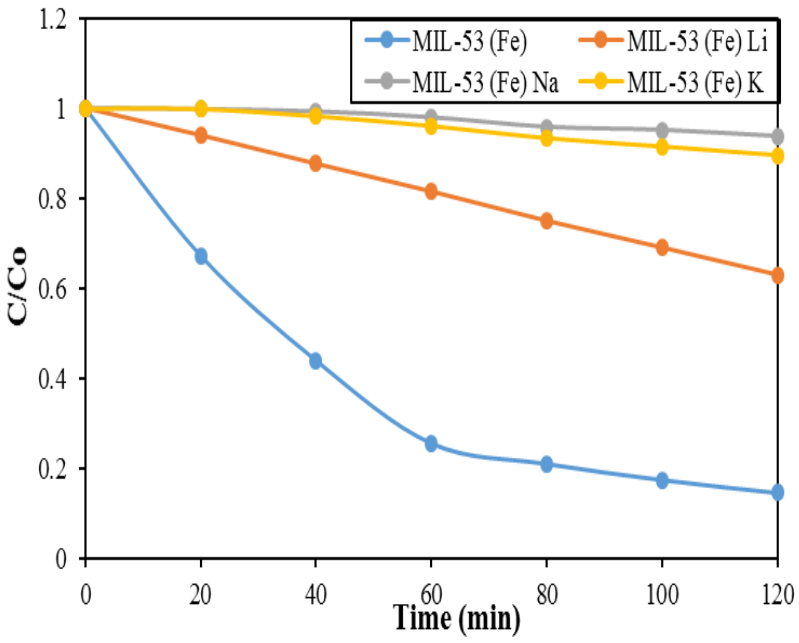

Figure 4.9: Photo degradation of MB dye over MIL-53 (Fe), MIL-53 (Fe) Li doped, MIL-53 (Fe) Na doped, MIL-53 (Fe) K doped.

From the Figure 4.9, it could be inferred that all the doped variants show photocatalytic activity in presence of artificial light. The order of photocatalytic activity decreases in MIL-53(Fe) > MIL-53(Fe) Li> MIL-53(Fe) K> MIL-53(Fe) Na.

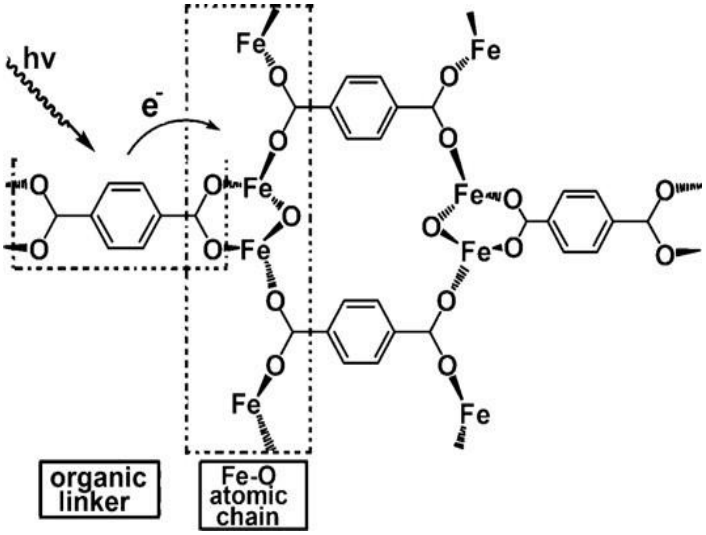

Figure 4.10: The structure of MIL-53(Fe) and the mechanism of electron transfer processes that occur in MIL-53(Fe) after irradiation.

Courtesy : J.-J. Du et al. / Journal of Hazardous Materials *190 (2011) 945–951*

The photocatalytic activity of MIL-53 (Fe) and its doped variants is reported in photodegradation of methylene blue dye. Figure 4.10 shows structure of MIL-53 (Fe) and dye degradation mechanism. It is understood from above the figure that MIL-53 (Fe) is porous crystalline material built up by infinite one dimensional linkage of –Fe–O–O–Fe–O–Fe– cross linked with BDC linkers. As the material, along with dye, is irradiated to UV-vis or visible light, electron excitation occur which cause transfer of electron and hole formation. The generation of holes being a reducing strength oxidizes the dye. Electron accepters when added to the system enhances the rate of reaction by generation of radicals and suppression of electron-hole recombination. Hence the synergic effect of enhancer additive has been studied.

Table 4.3: Results of test for Photosensitivity of dyes

Sr. No.	Substrate Name	Classification	Structure	maximum Wavelength	Photosensitivity [Appendix II]	Reference
1	Methylene Blue	Basic-Cationic	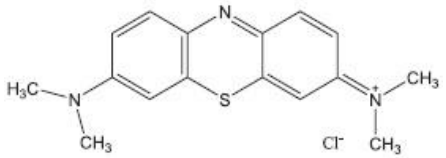	664 nm	Photoresistive	[18]
2	Congo Red	Diazo-cationic	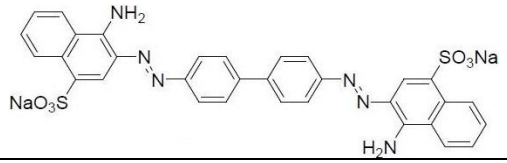	500 nm	photosensitive	[19]
3	Brilliant Green	Triarylmethane -cationic	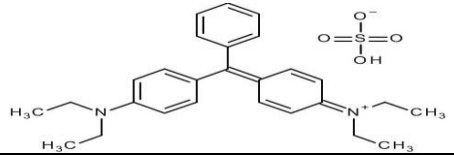	625 nm	photoresistive	[20]
4	Remazol Golden Yellow	Diazo-Anionic	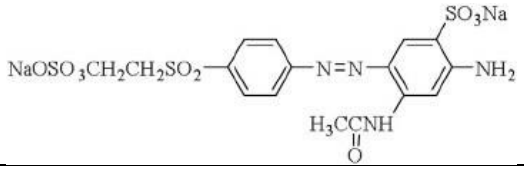	415 nm	Photoresistive	[21]
5	Trypan Blue	Diazo-Anionic	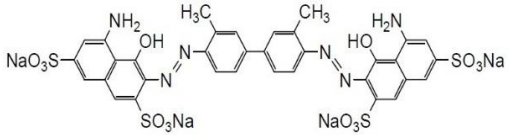	601 nm	photoresistive	[22]
6	Amido Black	Diazo-Anionic	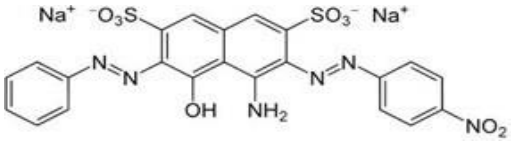	617 nm	Photoresistive	[23]

4.5 Photodegradation of BG dye using synthesized material

Figure 4.11 and 4.12 shows the reaction kinetics of photodegradation using 4 catalysts with and without electron acceptor. Results clearly depict that reaction rate for MIL-53(Fe) > MIL-53(Fe) Li > MIL-53(Fe) K > MIL-53(Fe) Na.

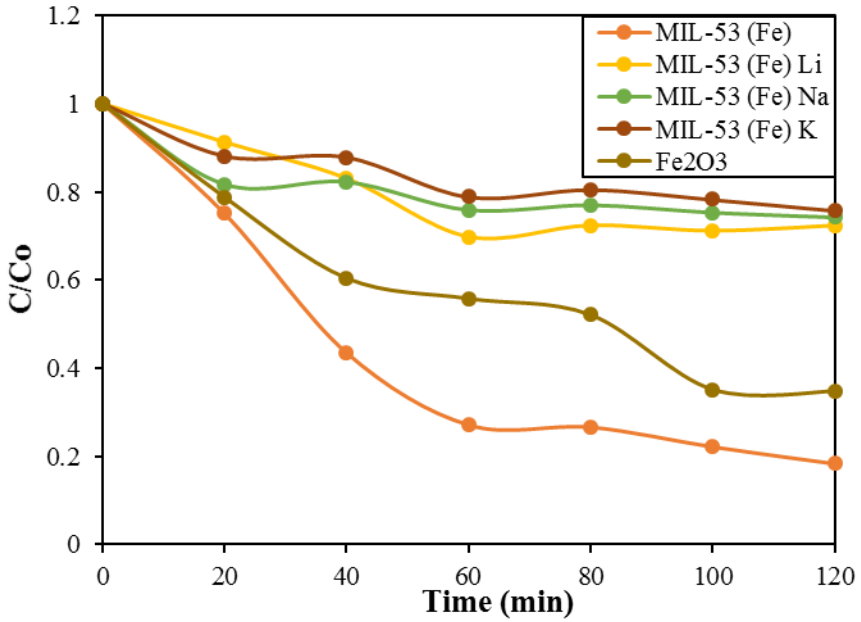

Figure 4.11: Kinetics of photodegradation of BG dye over catalyst

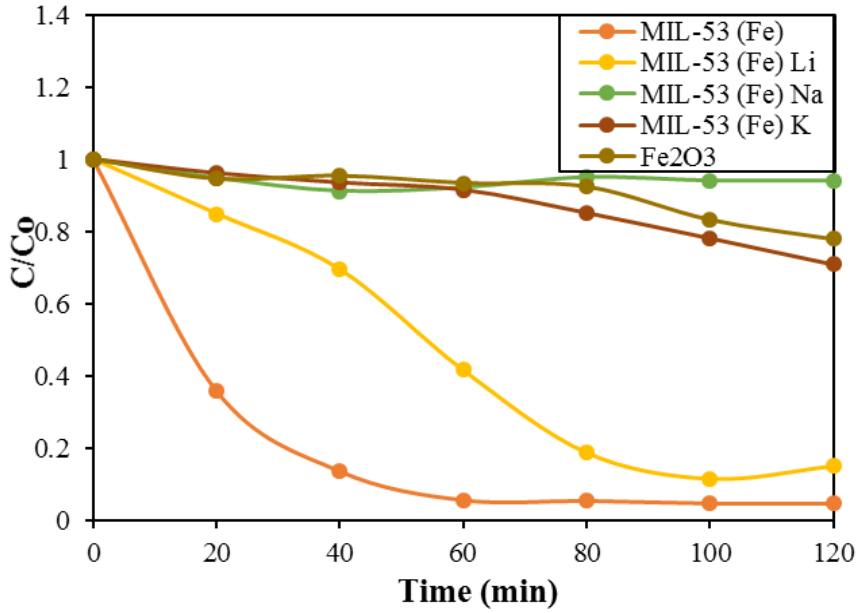

Figure 4.12: Kinetics of photodegradation of BG dye over catalyst + enhancer

Figure 4.11 and 4.12 in conflation show the effect of additive enhancer on the rate of reaction. This effect of enhancer on reaction rate can be calculated numerically by Synergy Index. Synergy index (SI), indicates a synergic effect for the photocatalytic process over MIL-53(Fe) photocatalyst in the presence of electron acceptor additives and is defined as,

$$\mathbf{SI} = \frac{\mathbf{K}_{(\text{enhancer+MIL}-53\,(\text{Fe}))}}{\mathbf{K}_{(\text{enhancer})} + \mathbf{K}_{(MIL-53\,(\text{Fe}))}} \quad \ldots\ldots\ldots\ldots\ldots (4.3)$$

SI for MIL-53(Fe), MIL-53(Fe) Li, MIL-53(Fe) Na, MIL-53(Fe) K are calculated as 2.2, 4.25, 0.2, and 0.75 respectively. Hence after addition of electron acceptor MIL-53 (Fe) and MIL-53(Fe) Li give better degradation gave motivation for the optimization of photodegradation of BG dye over MIL-53 (Fe) and MIL-53(Fe) Li catalyst.

4.6 Optimization of degradation of BG dye over MIL-53 (Fe)

From the Figure 4.13, ANOVA shows the relationship between parameters and system response via main effect plot. The best combination obtained by optimization was found at 10 ppm of BG dye concentration, 10 mg of MIL-53 (Fe) catalyst and 10 mM H_2O_2 enhancer concentration. The degradation efficiency was about 96%.

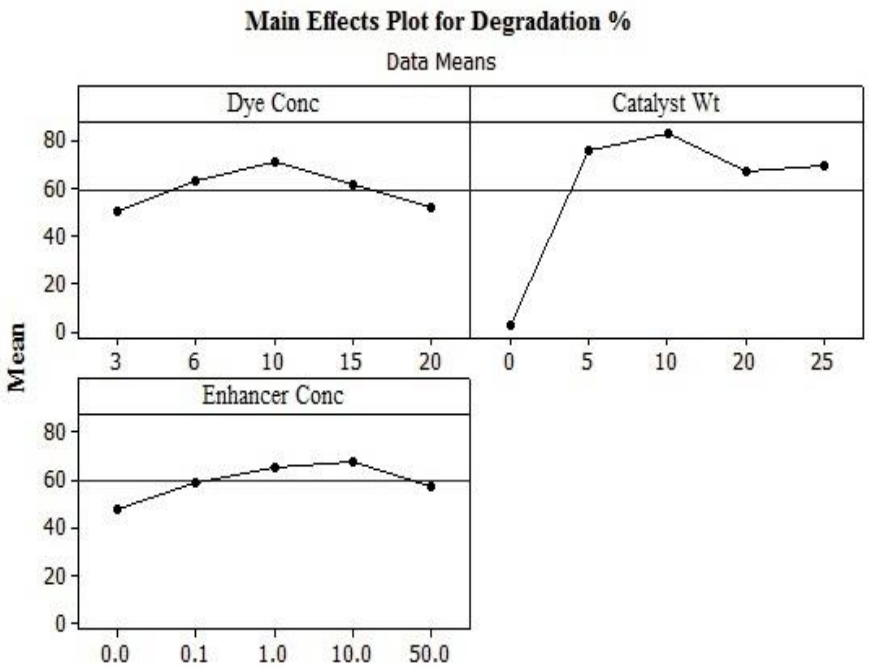

Figure 4.13: Main effects plot for degradation percentage

Table 4.4: Results of Optimization table for degradation of BG dye over MIL-53 (Fe)

dye conc. (ppm)	catalyst wt. (mg)	H_2O_2 conc. (m M)	% Degradation	k_{avg} min^{-1}	R^2	SI
3	0	0	0	0	-	-
3	5	0.1	89.231	0.0062	0.9651	0.29
3	10	1	96.623	0.0056	0.9807	0.26
3	20	10	82.682	0.0164	0.8575	0.76
3	25	50	80.928	1.5780	0.9832	-
6	0	0.1	0	0	-	-
6	5	1	91.363	0.0168	0.9863	0.78
6	10	10	98.109	0.0572	0.997	2.64
6	20	50	91.108	2.3460	0.9928	-
6	25	0	89.248	0.0514	0.9784	2.36
10	0	1	10.997	0	-	-
10	5	10	98.285	0.0475	0.9998	2.19
10	10	50	94.308	0.0427	0.9894	1.96
10	20	0	92.317	0.0301	0.9806	1.39
10	25	0.1	95.762	0.0403	0.9691	1.85
15	0	10	8.409	0.1266	0.7339	5.83
15	5	50	93.117	0.0188	0.9991	0.87
15	10	0	83.049	0.0282	0.9997	1.29
15	20	0.1	89.088	0.0291	0.9951	1.34
15	25	1	93.804	0.0322	0.9347	1.48
20	0	50	0	0	-	-
20	5	0	52.058	0.0227	0.8627	1.05
20	10	0.1	84.259	0.0233	0.9491	1.07
20	20	1	91.336	0.0145	0.9808	0.67
20	25	10	97.627	0.0396	0.9985	1.82

Figure 4.14: Showed, degradation increases with increase in catalyst weight and enhancer concentration. Degradation is decreasing below 5 mg catalyst weight as dye concentration increases. Figure 4.15 showed, addition of enhancer in the system will improve the reaction rate at even in presence of less amount of catalyst i.e. 5 mg.

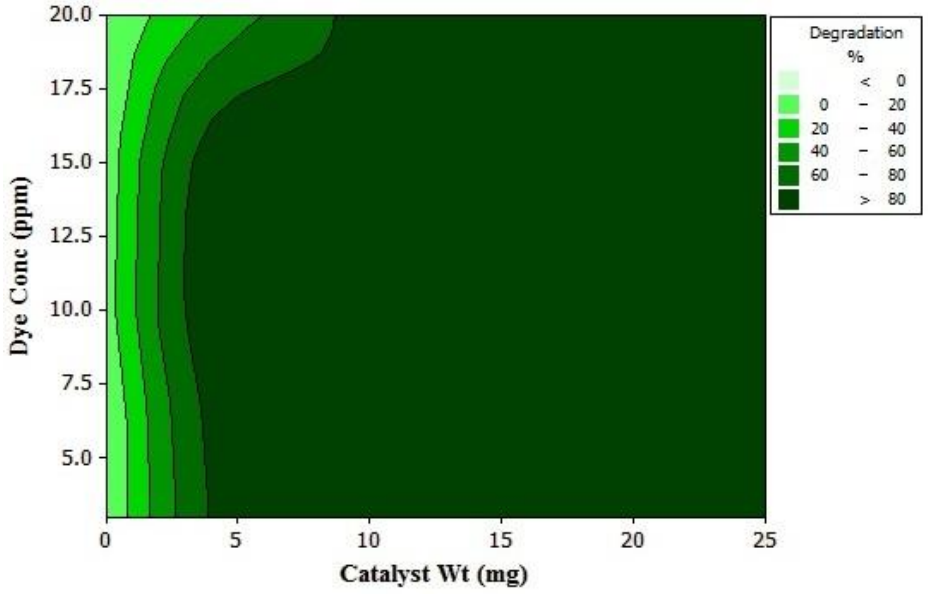

Figure 4.14: Counterplot of BG dye degradation with respect to dye concentration and catalyst weight

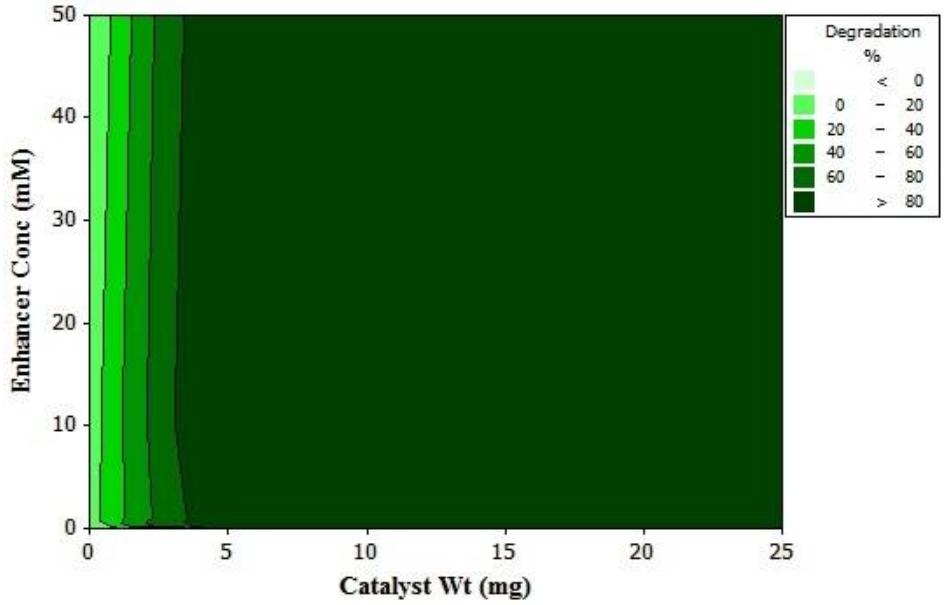

Figure 4.15: Counterplot of BG dye degradation with respect to Enhancer concentration and catalyst weight.

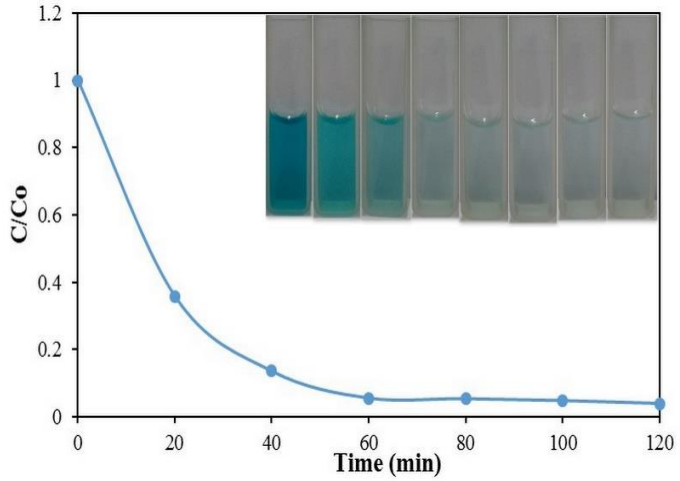

Figure 4.16: Concentration vs time data with photographical view of best combination.

Best results were obtained at 10 ppm dye concentration, 10 mg catalyst (MIL-53 (Fe)) and 10 mM electron acceptor (H_2O_2) giving 96 % degradation and 2.2 synergic index.

4.7 Optimization of degradation of BG dye over Li doped MIL-53 (Fe)

High senergic effect of enhancer on the system of dye degradation over Li doped MIL-53 (Fe) motivated to do the optimization of the same process. From the Figure 4.17, ANOVA shows the relationship between parameters and system response via main effect plot which specified the best degradation of BG dye at low dye concentration, Catalyst weight in between 10 mg to 20 mg and higher enhancer concenration.

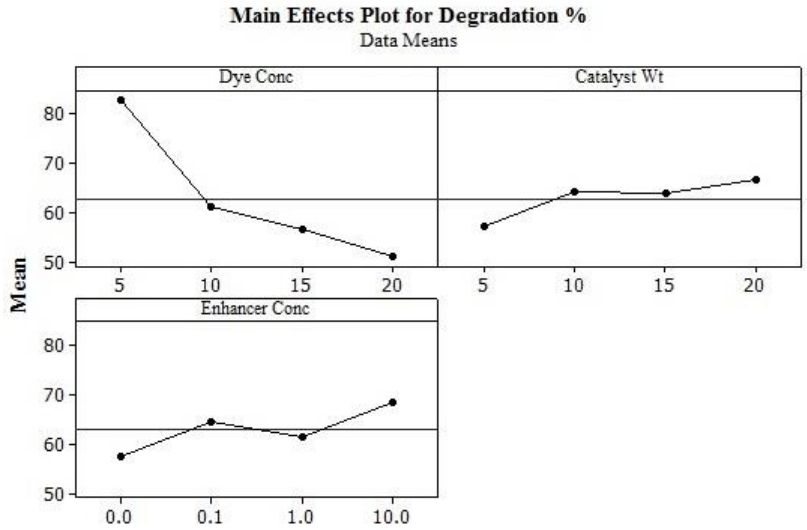

Figure 4.17: Main effect plot for drgradation percentage

Table 4.5: Results of Optimization table for degradation of BG dye over Li doped MIL-53 (Fe)

dye conc. (ppm)	catalyst wt. (mg)	enhancer conc. (m M)	degradation %	k min^{-1}	R^2	SI
5	5	0	69.914	0	0.9947	0
5	10	0.1	92.207	0.0155	0.9864	3.88
5	15	1	81.194	0.0083	0.9925	2.07
5	20	10	88.060	0.0154	0.9815	3.85
10	5	0.1	54.533	2.3730	0.4831	-
10	10	0	54.478	0.0032	0.9642	0.814
10	15	10	69.420	0.0291	0.9915	7.28
10	20	1	66.632	0.0027	0.97	0.67
15	5	1	49.467	0.0038	0.8338	0.94
15	10	10	61.513	0.0521	0.9994	13.01
15	15	0	54.614	0	0.9621	0
15	20	0.1	60.880	0	0.8964	0
20	5	10	54.825	0.0849	0.9817	21.22
20	10	1	48.118	0.0166	0.8016	4.15
20	15	0.1	50.870	0	0.9562	0
20	20	0	50.994	0	0.8034	0

Baeutiful counter plots for this optimization are shown in figure 4.18, 4.19, 4.20.

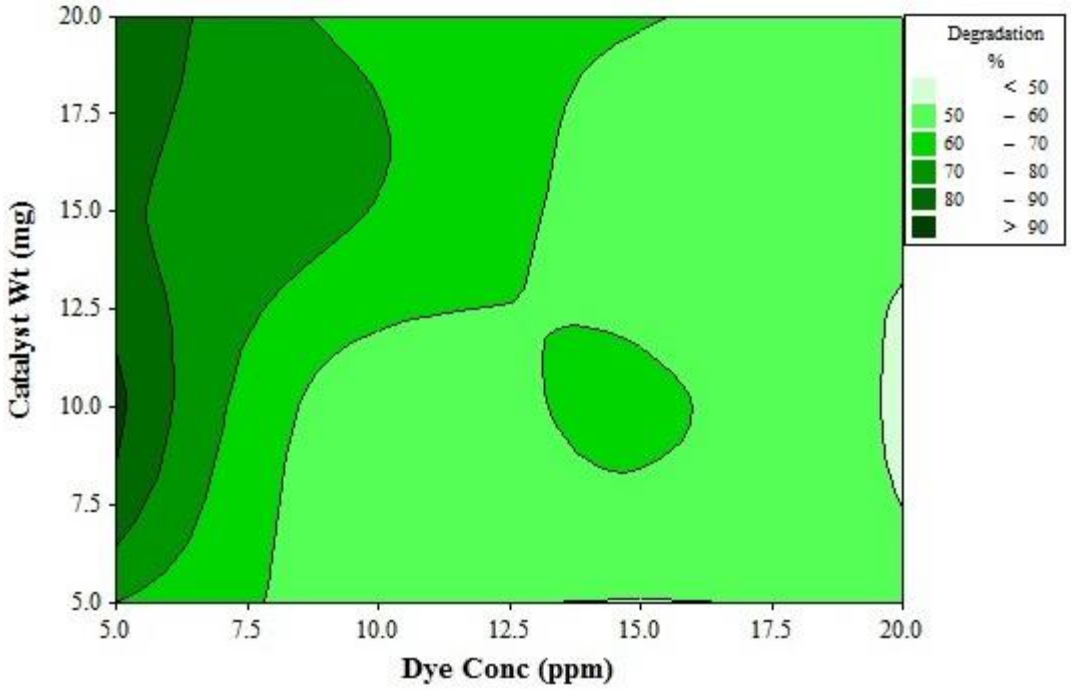

Figure 4.18: Counterplot of BG dye degradation with respect to dye concentration and catalyst weight

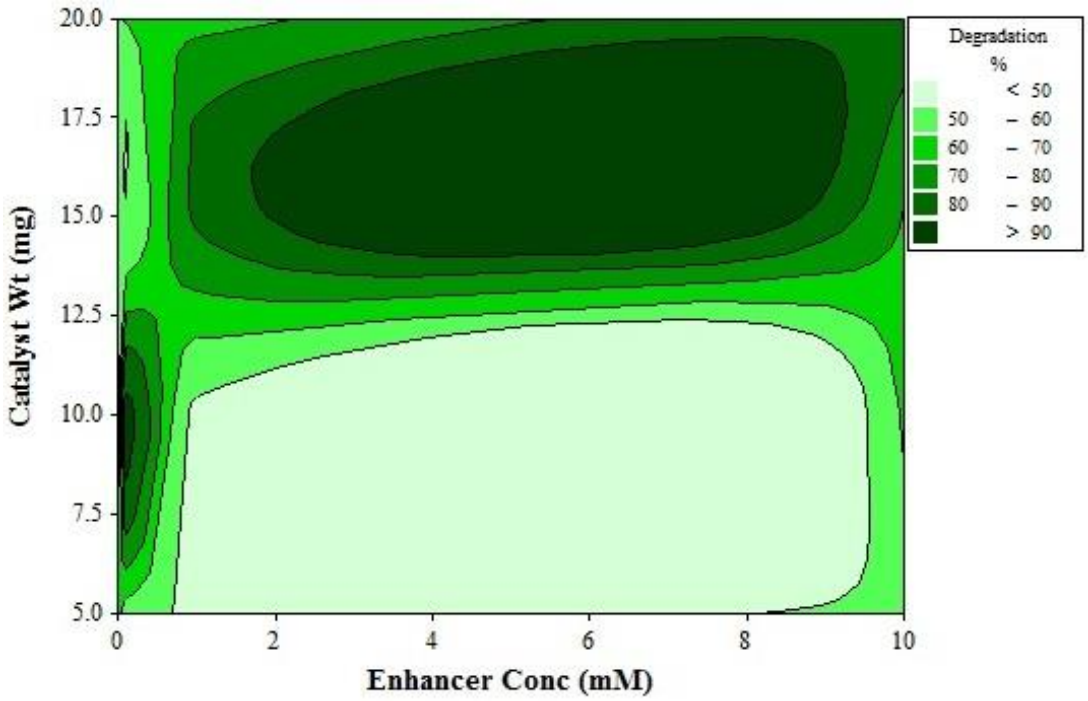

Figure 4.19: Counterplot of BG dye degradation with respect to Enhancer concentration concentration and catalyst weight

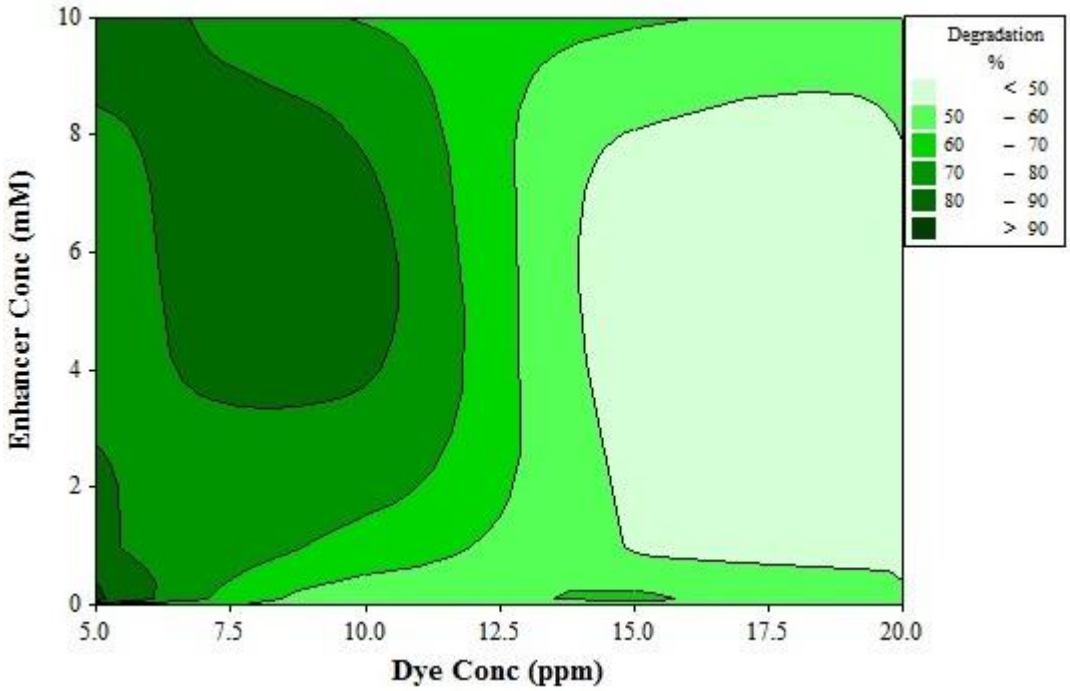

Figure 4.20: Counterplot of BG dye degradation with respect to dye concentration and enhancer concentration

This three counter plots show the effect of dye concentration, catalyst weight and enhancer concentration on the whole reaction system. These plot combinly showed that best degradation can be obtained at low dye concentration, high catalyst weight and high enhancer concentration.

CHAPTER 5

CONCLUSIONS AND FUTURE SCOPE

This work highlights successful synthesis of MIL-53 (Fe) metal organic framework and its doped derivatives (Li, Na, K) using microwave technique. Various characterization techniques like SEM, PXRD, TGA and UV-Vis reflectance detailed the physical, thermal and electronic properties of the synthesized materials and the results corroborated with reported literature. MIL-53 (Fe) was found to be stable up to 330°C and fairly stable in aqueous environment where pH was ranging from 2-11. Its cation doped variants were also found to be photocatalytically active and the activity decreased in the following order: MIL-53(Fe) > MIL-53(Fe) Li> MIL-53(Fe) K> MIL-53(Fe) Na; both in presence as well as in absence of an electron acceptor (H_2O_2). Finally, MIL-53 (Fe) showed degradation efficiency of approximate 86% and in presence of H_2O_2 as an enhancer it increased to 96%.

Future scope may go through optimization of Photodegradation if BG dye over MIL-53 (Fe) at various pH. Work done is based on a cationic dye but anionic dye may give good results as synthesized MOFs are cation doped. Recyclability of MIL-53 (Fe) after multiple degradation cycles can also be investigated.

References

1. Farrusseng D., Aguado S., and Pinel C., "Metal–Organic Frameworks: Opportunities for Catalysis", *Gesellschaft Deuscher Chemiker,* DOI: 10.1002/anie.200806063.
2. Lin C. K., Zhao D., Gao E. Y., Yang Z., Ye J., Xu T., Ge Q., Ma S., Lui D. J., "Tunability of Band Gaps in Metal Organic Frameworks", *Inorganic Chemistry*, 51. 9039-9044 (2012).
3. Mills A., Hunte S. L., "An overview of semiconductor photocatalysis", *Photochemistry and Photobiology A: Chemistry* 108 (1997) 1-35.
4. Ohtani B., "Photocatalysis A to Z-What we know and what we do not know in a scientific sense", *Photochemistry Reviews* 11 (2010) 157–178.
5. Korake P. V., Achary S. N., Gupta N. M., "Role of aliovalent cation doping in the activity of nanocrystalline CdS for visible-light-driven H2 production from water", *International journal of hydrogen energy*, 40 (2015) 8695 e8705.
6. Garcia H., Francese X. L. X., and Corma A. "Applications of Metal Organic Frameworks as quantum dots semiconductors", *Journal of Phisical Chemistry C* 111, 80-85 (2007).
7. Natarajan S., Mahata P., and Madras G., "Novel Photocatalysts for the Decomposition of Organic Dyes Based on Metal-Organic Framework Compounds", *Journal of Phisical Chemistry* B 2006, 110, 13759-13768.
8. Zhang Y., Li G., Lu H., Lva Q., and Suna Z., "Synthesis, characterization and photocatalytic properties of MIL-53(Fe)-graphene hybrid materials", *Royal Society of Chemistry Adv*ance, 2014, 4, 7594.
9. Alvaro M., Carbonell E., Ferrer B., Xamena F. X. L., Garcia H., "Semiconductor Behavior of a Metal-Organic Framework (MOF)", *Chemistry, A European journal*, DOI:10.1002/chem.200601003
10. Fu Y., Chen D. S. Y., Huang R., Ding Z., Fu X., Li Z., "An Amine-Functionalized Titanium Metal–Organic Framework Photocatalyst with Visible-Light-Induced Activity for CO_2 Reduction", *Journal of the Gesellschaft Deuscher Chemiker*, DOI: 10.1002/ange.201108357.

11. Du J. J., Yuan Y. P., Sun J. X., Peng F. M., Jiang X., Qiu L. G., Xie A. J., Shen Y. H., Zhu J. F., "New photocatalysts based on MIL-53 metal-organic frameworks for the decolorization of methylene blue dye", *Journal of Hazardous Materials* 190 (2011) 945–951.
12. Haque E., Khan N. A., Park J. H., and Jhung S. H., "Synthesis of a Metal–Organic Framework Material, Iron Terephthalate, by Ultrasound, Microwave, and Conventional Electric Heating: A Kinetic Study", DOI: 10.1002/chem.200902382.
13. Zhou T., Du Y., Borgna A., Hong J., Wang Y., Han J., Zhang W., and Xu R., "Post-synthesis modification of a metal–organic framework to construct a bifunctional photocatalyst for hydrogen production", *Energy Environmental Science*, 2013, 6, 3229-3234.
14. Dong W., Liu X., Shi W., and Huang Y., "Metal–organic framework MIL-53(Fe): facile microwave-assisted synthesis and use as a highly active peroxidase mimetic for glucose biosensing", *Royal Society of Chemistry Advance*, 2015, 5, 17451.
15. Nguyen M. T. H., NguyenQ. T., "Efficient refinement of a metal–organic framework MIL-53(Fe) by UV–vis irradiation in aqueous hydrogen peroxide solution", *Photochemistry and Photobiology A: Chemistry* 288 (2014) 55–59.
16. Serpone N., "Is the Band Gap of Pristine TiO2 Narrowed by Anion- and Cation-Doping of Titanium Dioxide in Second-Generation Photocatalysts?", *Journal of Physical Chemistry*, B 2006, 110, 24287-24293.
17. Herrmann J. M., "Heterogeneous photocatalysis: fundamentals and applications to the removal of various types of aqueous pollutants", *Catalysis Today* 53 (1999) 115–129.
18. Haque E., Jun J. W., Jhung S. H., "Adsorptive removal of methyl orange and methylene blue from aqueous solution with a metal-organic framework material, iron terephthalate (MOF-235)", *Journal of Hazardous Materials*, 185 (2011) 507–511.
19. Mondal K., and Sharma A., "Photocatalytic Oxidation of Pollutant Dyes in Wastewater by TiO2 and ZnO nano-materials – A Mini-review."
20. Rehman R., Mahmud T., Irum M., "Brilliant Green Dye Elimination from Water Using Psidium guajava Leaves and Solanum tuberosum Peels as Adsorbents in Environmentally Benign Way", *Journal of Chemistry*, Volume 2015, Article ID 126036.

21. Bi X., Wang P., Jiao C., Cao H, "Degradation of remazol golden yellow dye wastewater in microwave enhanced ClO_2 catalytic oxidation process", *Journal of Hazardous Materials.*, 168 (2009) 895-900.
22. Anantha N., Rao S., Venkataraghngaiah V. T., "Electrochemical treatment of Trypan Blue synthetic wastewater and its degradation pathway", *Journal of Electrochemical Science and Engineering*, (2013) 167-184.
23. Ma F., Liang S., Peng Y., Kuang Y., Zhang X., Chen S., Long Y., Zeng R., "Copper ion detection using novel silver nanoclusters stabilized with amido black 10B", Analytical and Bioanalytical Chemistry, May 2016, Volume 408, Issue 12.
24. Ravindran A., Reklaitis G. V., Ragsdell K. M., "Engineering optimization: methods and applications".

APPENDIX I

Preparation of Standard Organic Dye Solutions

Preparation of Methylene blue standard solution

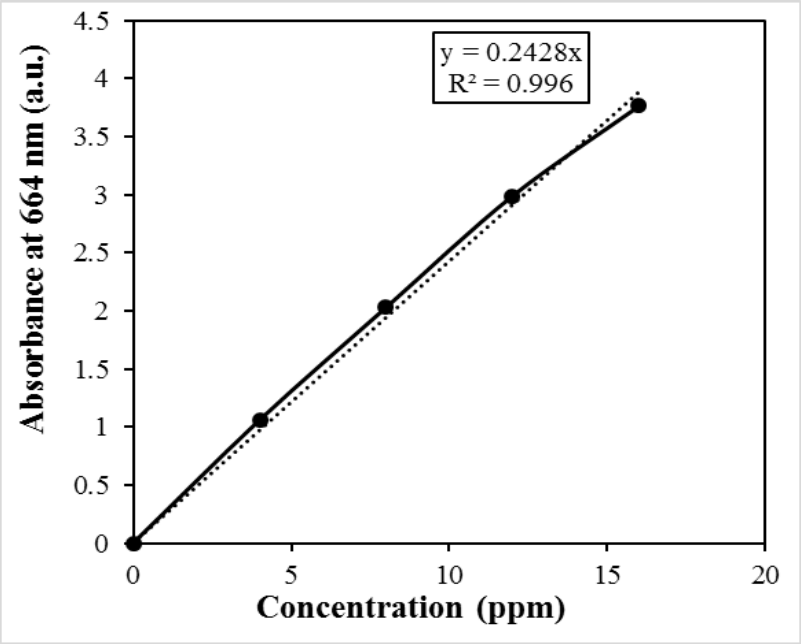

Figure I.A: standard curve of Methylene Blue dye solution

Preparation of Brilliant Green standard solution

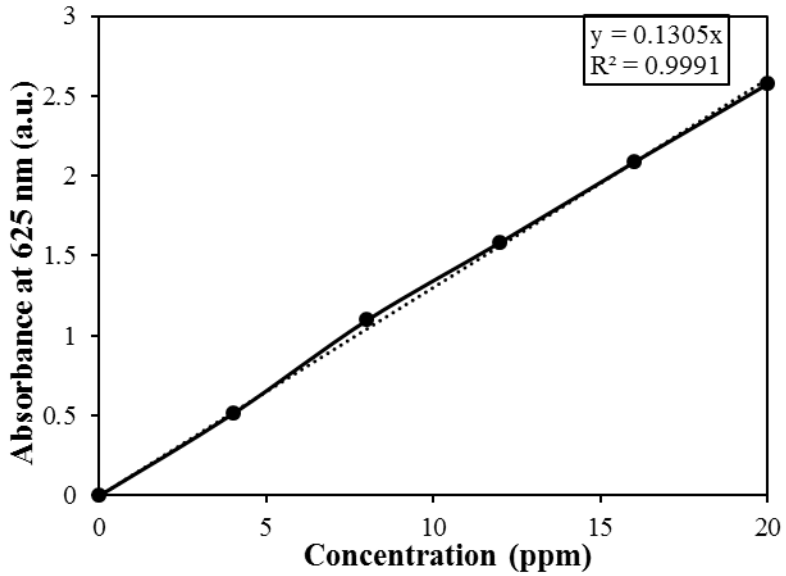

Figure I.B: standard curve of Brilliant Green dye solution

Preparation of Congo red standard solution

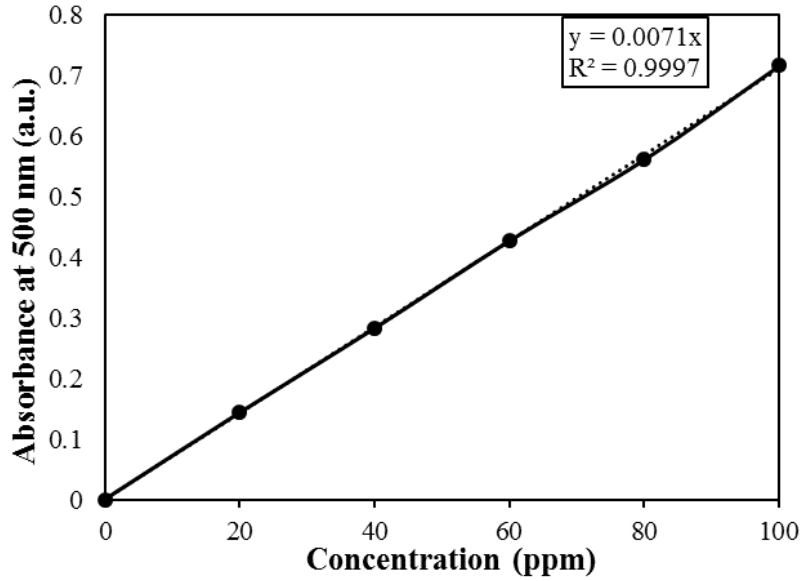

Figure I.C: standard curve of Congo Red dye solution

Preparation of Remazol Golden Yellow standard solution

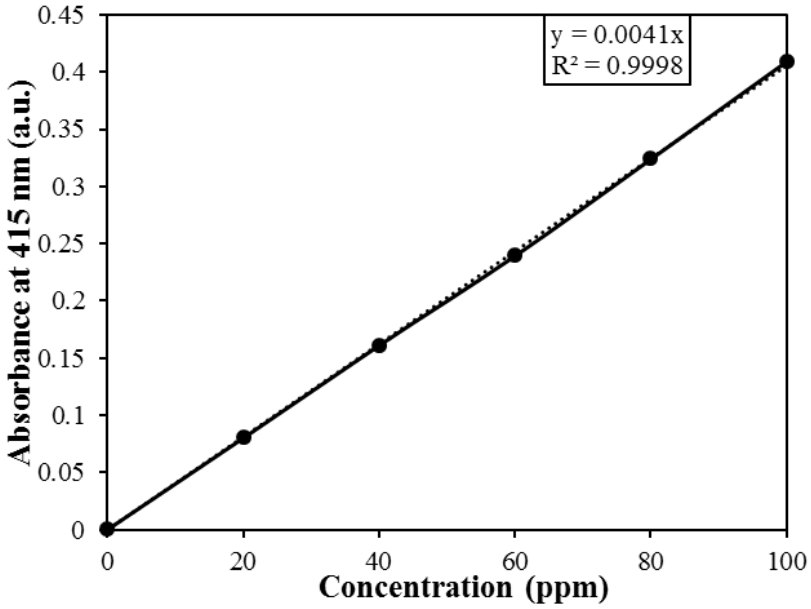

Figure I.D: standard curve of Congo Red dye solution

APPENDIX II

Study of Photosensitivity of organic dyes

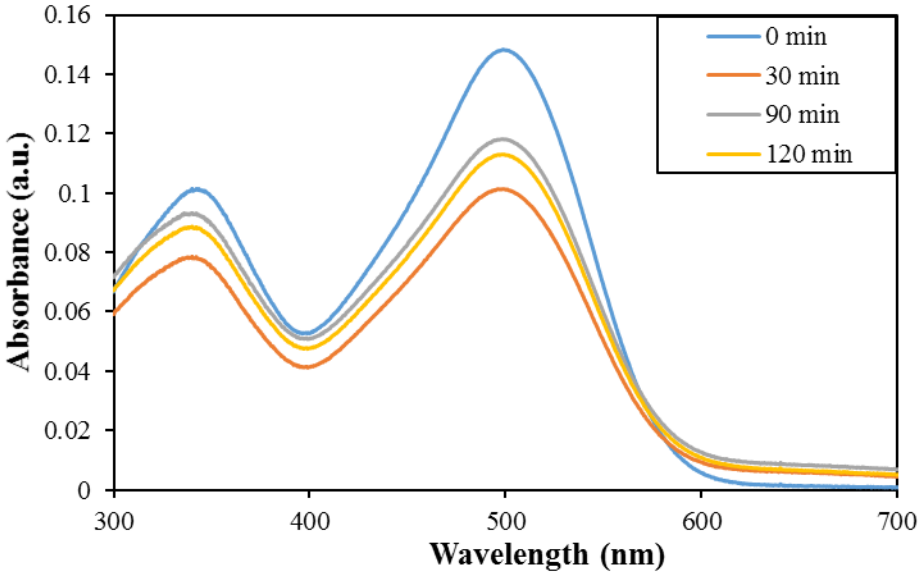

Figure II.A: Spectroscopic view photosensitivity of Congo Red dye solution

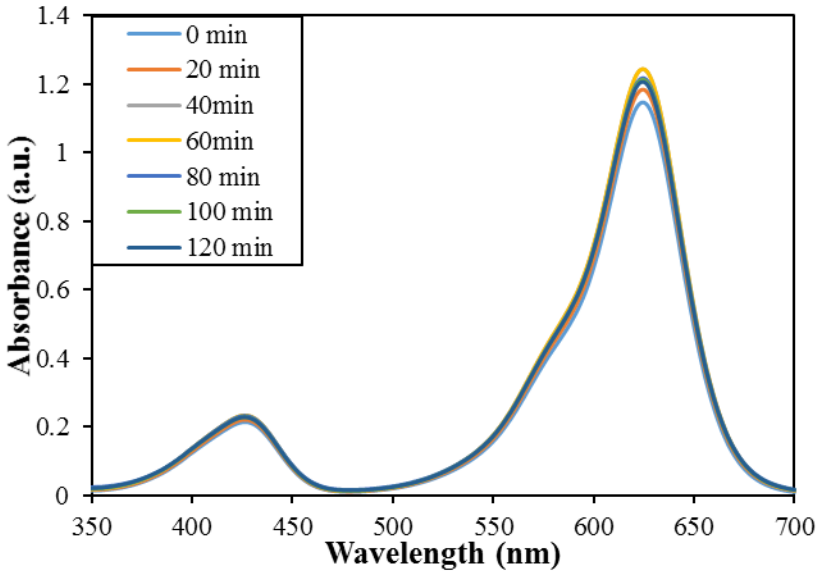

Figure II.B: Spectroscopic view photosensitivity of Brilliant Green dye solution

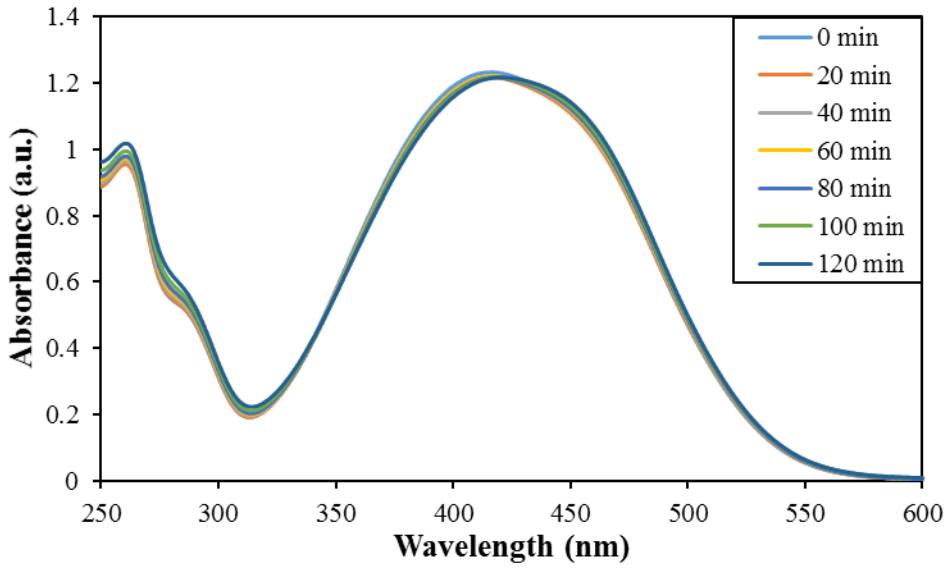

Figure II.C: Spectroscopic view photosensitivity of Remazol Golden Yellow dye solution

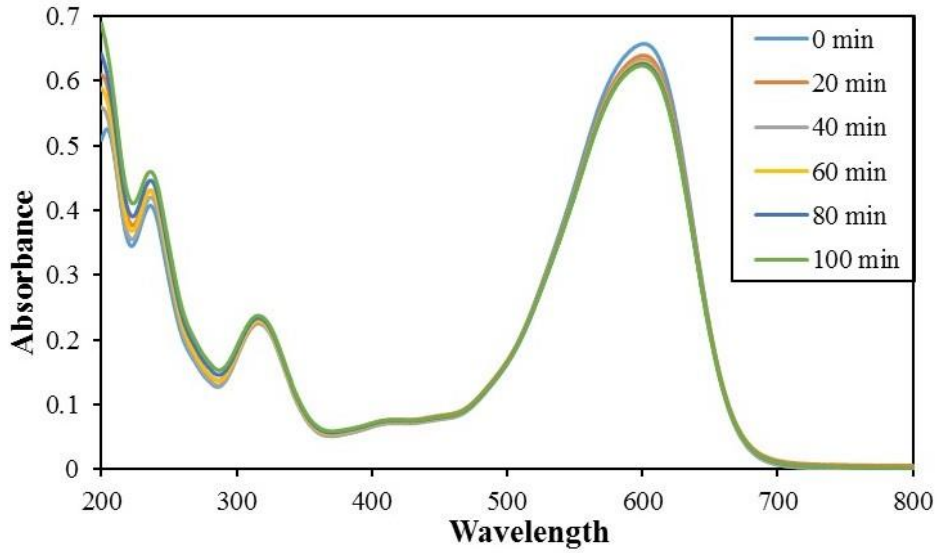

Figure II.D: Spectroscopic view photosensitivity of Trypan Blue dye solution

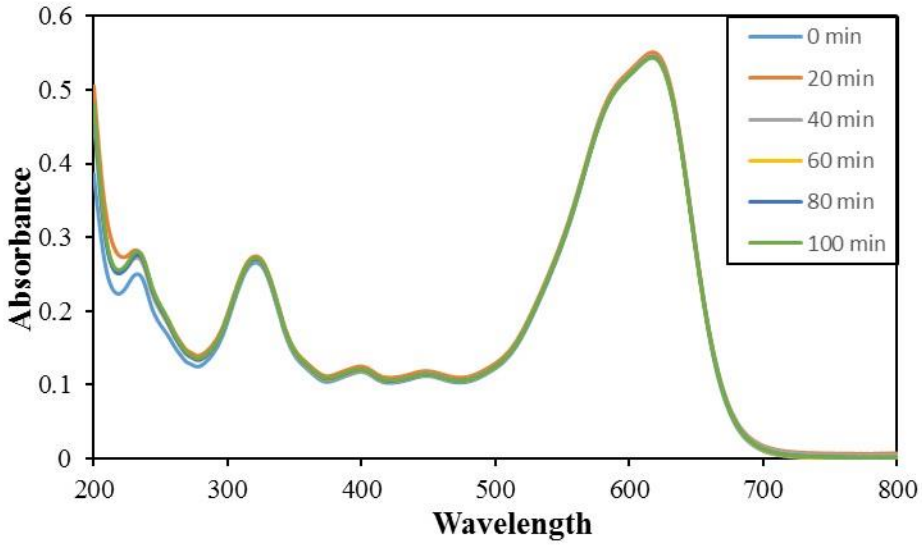

Figure II.E: Spectroscopic view photosensitivity of Amido Black dye solution

APPENDIX III

Optimization for photodegradation of BG dye over MIL-53 (Fe)

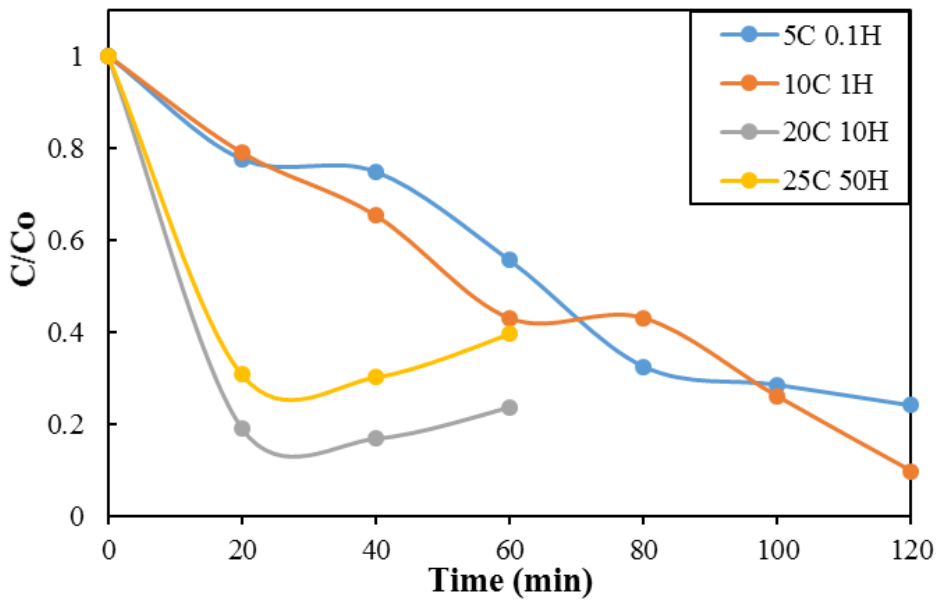

Figure III.A: Kinetics of optimization at 3 ppm BG dye solution

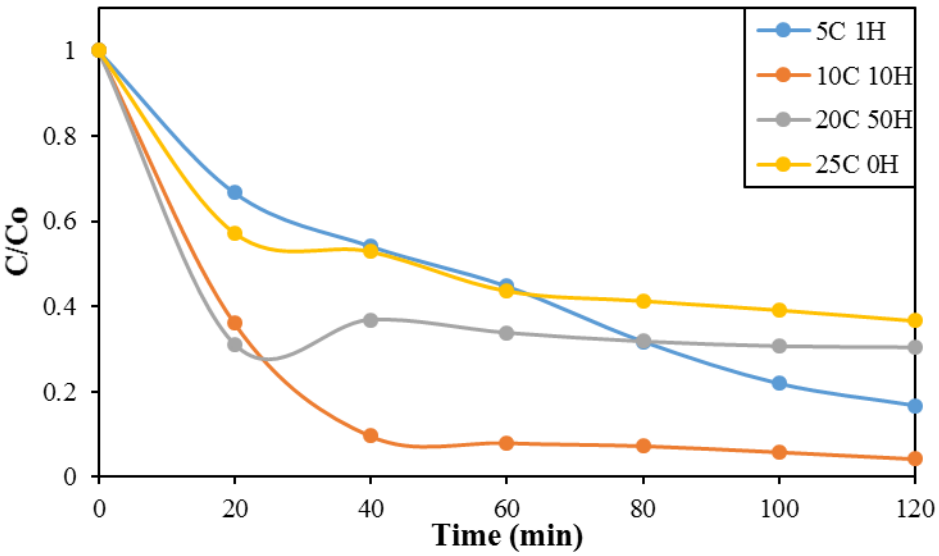

Figure III.B: Kinetics of optimization at 6 ppm BG dye solution

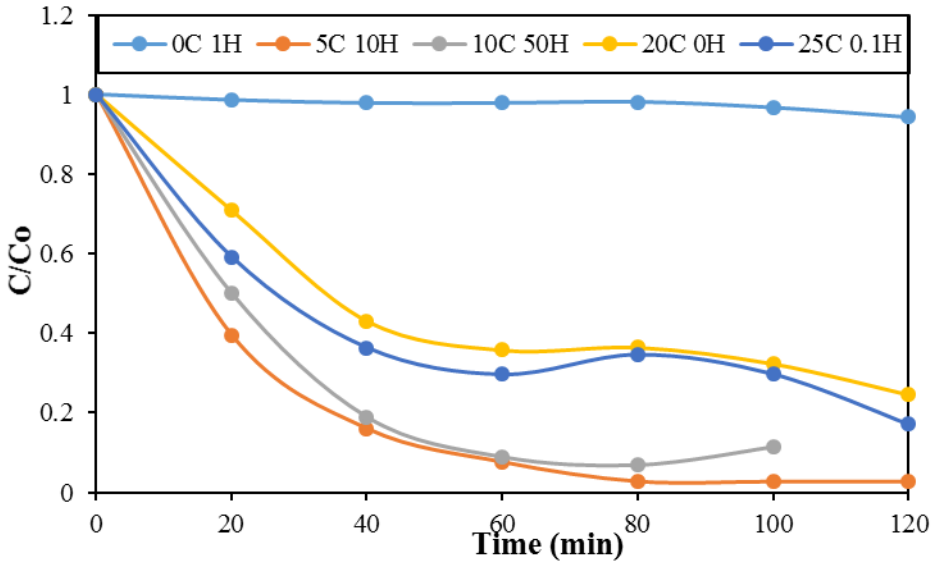

Figure III.C: Kinetics of optimization at 10 ppm BG dye solution

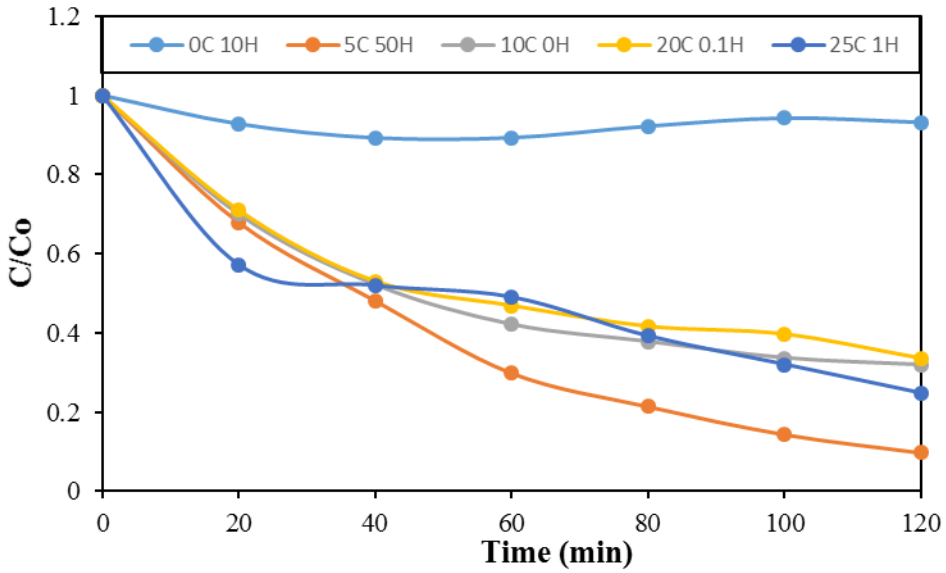

Figure III.D: Kinetics of optimization at 15 ppm BG dye solution

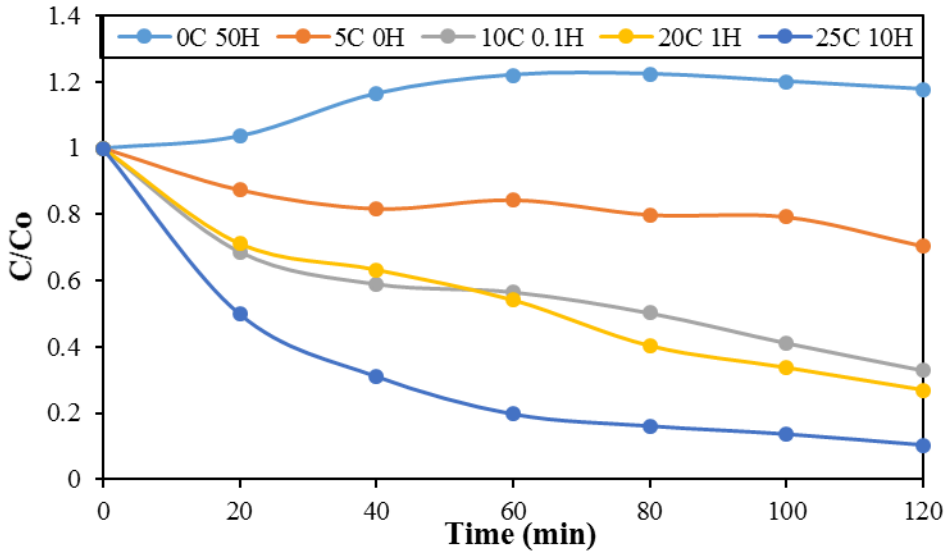

Figure III.E: Kinetics of optimization at 20 ppm BG dye solution

APPENDIX IV

Optimization for photodegradation of BG dye over Li doped MIL-53 (Fe)

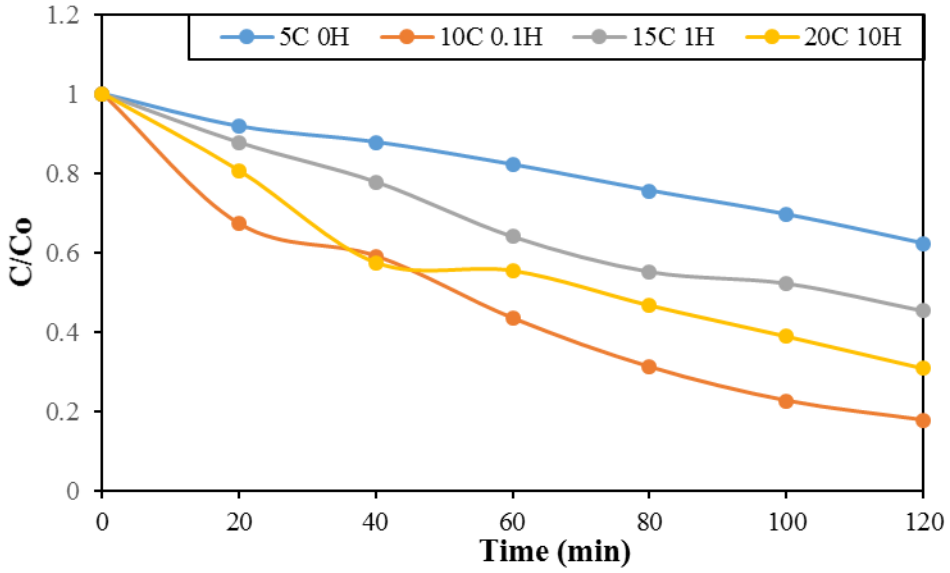

Figure IV.A: Kinetics of optimization at 5 ppm BG dye solution

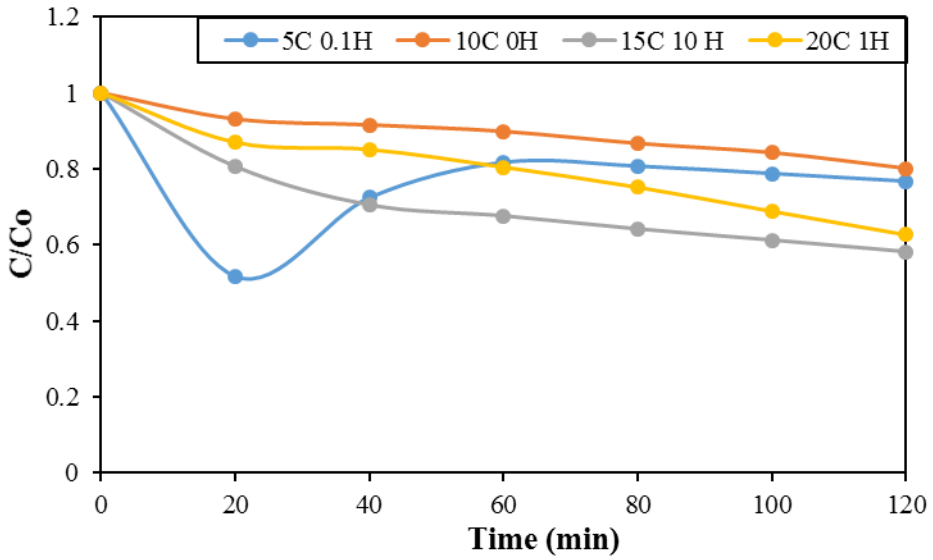

Figure IV.B: Kinetics of optimization at 10 ppm BG dye solution

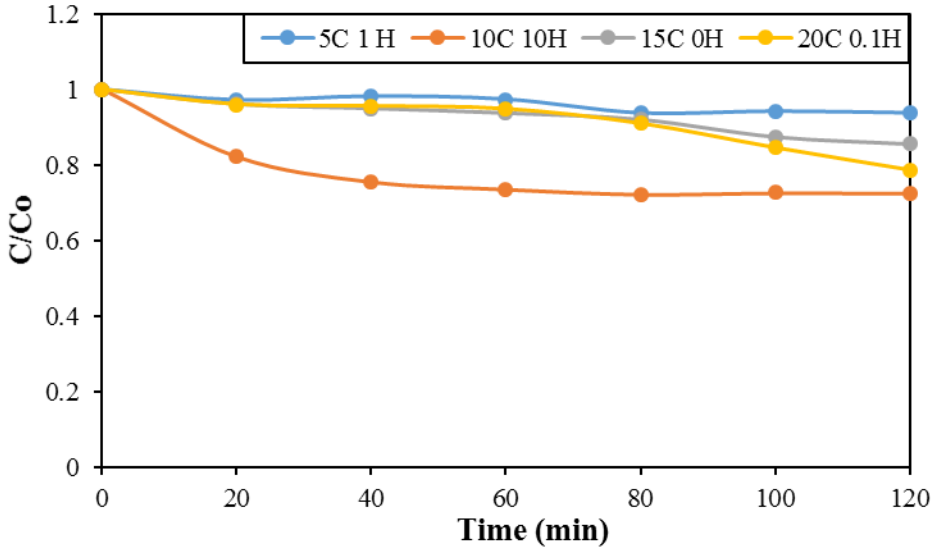

Figure IV.C: Kinetics of optimization at 15 ppm BG dye solution

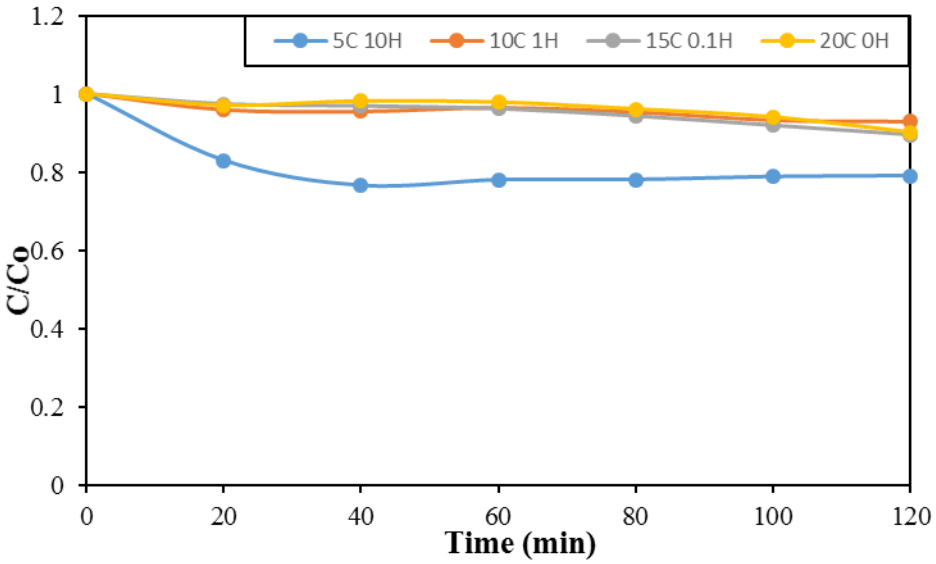

Figure IV.D: Kinetics of optimization at 20 ppm BG dye solution